Journal of Electrochemistry

Volume 28
Issue 7 *Special Issue on Electronic Electroplating (Ⅱ)*

2022-07-28

Electrodeposition of Functional Epitaxial Films for Electronics

Kui Huang

Rong-Jiao Huang

Su-Qin Liu

Zhen He
1. College of Chemistry and Chemical Engineering, Central South University, Changsha 410083, Hunan, China;2. Hunan Provincial Key Laboratory of Chemical Power Sources, Central South University, Changsha 410083, Hunan, China;, zhenhe@csu.edu.cn

Recommended Citation
Kui Huang, Rong-Jiao Huang, Su-Qin Liu, Zhen He. Electrodeposition of Functional Epitaxial Films for Electronics[J]. *Journal of Electrochemistry*, 2022 , 28(7): 2213006.
DOI: 10.13208/j.electrochem.2213006
Available at: https://jelectrochem.xmu.edu.cn/journal/vol28/iss7/5

电 化 学
J. Electrochem. 2022, 28(7), 2213006 (1 of 24)

[Review] DOI: 10.13208/j.electrochem.2213006 Http://electrochem.xmu.edu.cn

Electrodeposition of Functional Epitaxial Films for Electronics

Kui Huang[1], Rong-Jiao Huang[1], Su-Qin Liu[1,2], Zhen He[1,2*]

(*1. College of Chemistry and Chemical Engineering, Central South University, Changsha 410083, Hunan, China; 2. Hunan Provincial Key Laboratory of Chemical Power Sources, Central South University, Changsha 410083, Hunan, China*)

Abstract: Electrodeposition is a solution-based synthesis technique that can be used to fabricate various functional materials on conductive or semiconductive substrates under ambient conditions. Electrodeposition is usually triggered by an artificial electric stimulation (i.e., applied potential/current) to the substrate to oxidize or reduce ions, molecules, or complexes in the deposition solution layer near the substrate surface, which drives this solution layer to depart from its thermodynamic equilibrium and consequently causes the assembly of targeted deposits on the substrate. During electrodeposition, many experimental parameters could affect the properties of the deposits in different ways. To date, many elements (both metals and nonmetals), compounds (e.g., metal oxides, hydroxides, and chalcogenides), and composites have been electrodeposited, mostly as either polycrystalline, textured, or epitaxial films. Among them, the epitaxial films are a kind of single-crystal-like films grown with certain out-of-plane and in-plane orientations. Due to the highly ordered atomic arrangement in epitaxial films, they usually exhibit unique electric and magnetic properties. In this review, the common synthetic routes for the electrodeposition as well as the key experimental parameters that affect the epitaxial growth of the deposits are summarized. Besides, techniques used to characterize epitaxial films are briefly introduced. Furthermore, the electrodeposited functional epitaxial films with special electronic, electromagnetic, and photovoltaic properties are discussed.

Key words: electrodeposit; electroplating; thin film; highly oriented

1 Introduction

Electrodeposition, also known as electroplating, is a solution-based synthesis method that could be used to fabricate various functional materials of desired properties on conductive or semi-conductive solid surfaces (i.e., substrates). To date, various materials including metals, alloys, oxides, hydroxides, carbonates, and chalcogenides of different forms such as polycrystalline/textured/epitaxial films, porous networks, and special micro/nano-architectures (e.g., nanowires, nanorods, quantum dots, and superlattices) have been produced by electrodeposition. Although these materials with diverse structures could also be produced by other synthetic methods such as hydrothermal/solvothermal synthesis, chemical/physical vapor deposition, and reactive magnetron sputtering, electrodeposition offers several advantages over other synthetic approaches. First, electrodeposition is normally carried out under ambient conditions (i.e., under the standard pressure at/near room temperature), which makes it cost-effective and easily scalable[1]. The relatively low temperature of processing allows to fabricate materials, nanostructures, and interfaces that might not be stable at high temperatures[2] and endows electrodeposition with higher compatibility (compared to the aforementioned high-temperature/high-pressure synthetic methods) while integrated into the processing that has temperature con-

Cite as: Huang K, Huang R J, Liu S Q, He Z. Electrodeposition of functional epitaxial films for electronics. *J. Electrochem.*, 2022, 28(7): 2213006.

Received: 2022-02-28, Revised: 2022-05-04. *Corresponding author, Tel: (86-731)88879616, E-mail: zhenhe@csu.edu.cn

straints, such as the back-end-of-line (BEOL) processing for the integrated circuit (IC) manufacture [3]. Second, electrodeposition provides many degrees of freedom (e.g., composition, pH, temperature, and additives of the deposition bath, applied potential/current, and the substrates) in terms of tuning the properties of the targeted deposits[4]. Among these experimental variables, the applied potential and current on the substrate surface are two exclusive ones that are not applicable in other synthetic methods. Third, during electrodeposition, the deposits grow from the bottom up on the substrates, which guarantees a good electrical contact between the deposit and the substrate[2]. This feature is critical for device applications in electronics, and energy conversion and storage, such as the loading of active materials onto the current collectors in batteries and the formation of p-n junctions in photovoltaic devices. By virtue of these advantages, electrodeposition has been utilized or shown potential in fabricating many important components (either metals, alloys, compounds, or composites) with required electric, magnetic, and photovoltaic properties in electronics. For instance, copper electroplating is currently the prevailed interconnection technology in the manufacture of integrated circuits and printed circuit boards[5]. Besides, many ferri/ferromagnetic thin films of metals[6] and metal oxides [7, 8] with giant magnetoresistance (GMR) have been fabricated by electrodeposition and could be potentially used in electromagnetic and spintronic devices such as recording heads, magnetoresistive random access memories (MRAMs), magnetic sensors, and spin valves.

Various functional materials for electronics are commonly electrodeposited as polycrystalline, textured, or epitaxial films. Strictly speaking, epitaxial films refer to single-crystal layers that grow with the same crystallographic orientations as that of the substrates (which are mostly single crystals). However, in a more general definition, single-crystal-like films with growth orientations that are controlled by the substrate (but not necessarily the same as that of the substrate) are called epitaxial films. Compared to polycrystalline or textured films, epitaxial films (with a well-defined growth orientation to the substrate) usually possess fewer grain boundaries and defects, which allows better exploitation of the intrinsic properties of the materials and leads to superior device performance[9, 10]. Therefore, the fabrication of epitaxial films has currently attracted more and more attention. Although epitaxial films can be fabricated by various methods such as molecular beam epitaxy, chemical/physical vapor deposition, and reactive magnetron sputtering, the fabrication of epitaxial films by electrodeposition is more attractive due to its high accessibility and low cost.

Although there have been some reviews on electrodeposition, they mainly focused on polycrystalline films (rather than epitaxial films) used in electrodes[11], photoelectrodes [1], and batteries [12]. In addition, electrodeposited epitaxial ultrathin magnetic layers have been reviewed[13] with the emphasis on magnetic investigations. This review will focus on the electrodeposition, characterizations, and applications of epitaxial functional films for electronics. We will start with the discussion on the design of electrodeposition routes and control of growth orientations for the epitaxial films. Then, the characterization methods for the epitaxial films will be briefly introduced. Furthermore, various electrodeposited functional epitaxial films that could be used or potentially used in electronic, electromagnetic, and photovoltaic devices will be discussed.

2 Designs and Controls of Epitaxial Electrodeposition

To date, many functional materials have been synthesized by electrodeposition into the form of epitaxial films. Same as the common electrodeposition of any functional materials, to electrodeposit functional epitaxial films one would need to first design a synthetic route of electrodeposition that could trigger the nucleation and growth of the desired materials on the substrate surface. In addition, one should consider the factors that would affect the epitaxial growth of the electrodeposited functional films. In this section, we will first summarize some common synthetic routes

for the electrodeposition of different kinds of functional materials that could be used in electronics. Then, the key parameters that affect the epitaxial growth of the deposits during the electrodeposition will be discussed.

2.1 Common Synthetic Routes of Electrodeposition

Electrodeposition is triggered by an artificial electrical stimulation (i.e., the applied potential/current on the substrate) that could precisely control the solution layer near the substrate surface to deviate from its thermodynamic equilibrium. Although the electrical stimulation could be similar in electrodeposition, the triggers for the accumulation of different deposits on the substrate surfaces could be completely different. In general, the electrodeposition of metals/alloys usually involves only an electrochemical reaction, whereas the electrodeposition of compounds/composites commonly involves both electrochemical and chemical reactions[2]. Some common routes of electrodeposition are summarized as follows based on their different ways to trigger the deposition.

2.1.1 Direct Electrochemical Reduction of Ions to Their Atoms

The direct reduction of ions (M^{n+}, either in a coordinated or uncoordinated form) into their atoms (M) by driving the electrode potential on the substrate surface to a value that is more negative than the equilibrium potential of the corresponding redox couple, E (M^{n+}/M), could trigger the deposition of the corresponding elements on the substrate surface (Eq. 1). This mechanism is the most common one for electrodepositing metals and alloys[14]. It could also be used to electrodeposit nonmetallic elements such as carbon[15] and semiconductive elements such as germanium[16] and silicon[17].

$$M^{n+} + ne^- \rightarrow M \quad (1)$$

2.1.2 Changing Oxidation States of Ions

Ions (either as free cations/anions or in molecules/complex ions) in the deposition solution could be electrochemically oxidized or reduced by applying an electrode potential that is more positive or negative than the equilibrium potential of the corresponding redox couple. This electrochemical process involves electron transfer between the substrate surface and the corresponding electrochemically active species in the deposition solution. If the generated species is not the final product (unlike the electrodeposition of metals) and participates in the following chemical reactions to form the targeted deposit on the substrate, this whole process of electrodeposition follows an electrochemical-chemical (EC) mechanism. Such an EC mechanism is commonly seen in the electrodeposition of compounds[18-20]. For example, the electrodeposition of Fe_3O_4 has been achieved by electrochemically reducing Fe^{3+}-triethanolamine (TEA) to Fe^{2+} and TEA from an alkaline $Fe(TEA)^{3+}$ complex solution[18,21] (Eq. 2). Due to the much lower formation constant ($K^{\ominus}_f$) of the $Fe(TEA)^{2+}$ complex than that of the $Fe(TEA)^{3+}$ complex, the generated of Fe^{2+} is not stable in the strong alkaline solution, which then triggers the deposition of Fe_3O_4 through the following chemical reaction (Eq. 3). In addition to metallic cations, molecules in the solution could also be electrochemically reduced to anions to trigger the deposition following the EC mechanism. For instance, PbI_2 [22] and BiI_3[23] were electrodeposited by electrochemically reducing molecular iodine to iodide ions with the presence of the corresponding metal ions in the deposition solutions due to the small solubility-product constant ($K^{\ominus}_{sp}$) of these two metallic iodides (Eqs. 4 and 5).

$$Fe(TEA)^{3+} + e^- \rightarrow Fe^{2+} + TEA \quad (2)$$

$$Fe^{2+} + 2Fe(TEA)^{3+} + 8OH^- \rightarrow Fe_3O_4 + 2TEA + 4H_2O \quad (3)$$

$$I_2 + 2e^- \rightarrow 2I^- \quad (4)$$

$$M^{n+} + nI^- \rightarrow MI_n \quad (5)$$

2.1.3 Changing Local pH near Electrode Surface

The pH of the deposition solution near the electrode surface could be adjusted by electrochemical generation/consumption of acids or bases, which could be used as a trigger for the following chemical reactions. Thus, the electrodeposition triggered by the local pH change of the deposition solution near the electrode surface also follows the EC mechanism. The local pH change could be realized in different

ways, includin g the electrochemical reactions consuming H^+/OH^- ions or electrochemical oxidation/reduction of water and some other anions to generate acids/bases, which have been covered in detail in the literature [24]. Understandably, electrochemical base generation has been widely used to electrodeposit various metal oxides [25] and hydroxides [26, 27] (Eqs. 6 and 7). Besides, it could also be the trigger for the electrodeposition of other compounds such as $CaCO_3$ from a saturated $Ca(HCO_3)_2$ solution, in which the generated OH^- by electrochemical reduction of H_2O on the substrate surface (Eq. 8) reacts with HCO_3^- to produce CO_3^{2-} and triggers the $CaCO_3$ deposition (Eq. 9) [28]. The electrochemical generation of acids could be used to deposit amphoteric metal oxides from alkaline solutions. An example of it is the electrodeposition of ZnO by decreasing the local pH at the electrode surface via electrochemically oxidizing the ascorbate dianions (Eqs. 10-12)[29].

$$M^{n+} + nOH^- \rightarrow M(OH)_n \quad (6)$$

$$M^{n+} + nOH^- \rightarrow MO_{2/n} + H_2O \quad (7)$$

$$2H_2O + 2e^- \rightarrow H_2 + 2OH^- \quad (8)$$

$$OH^- + Ca^{2+} + HCO_3^- \rightarrow CaCO_3 + H_2O \quad (9)$$

$$C_6H_7O_6^{2-} + H_2O \rightarrow C_6H_8O_7 + H^+ + 2e^- \quad (10)$$

$$Zn(OH)_3^- + H^+ \rightarrow ZnO + 2H_2O \quad (11)$$

$$Zn(OH)_4^{2-} + 2H^+ \rightarrow ZnO + 3H_2O \quad (12)$$

2.1.4 Destruction of Protecting Ligands of Metal Ions

In many cases, metallic compounds could be produced by directly mixing the solutions containing the corresponding metal cations and anions. However, electrodeposition requires that the deposit forms only on the substrate surface rather than in the bulk solution. In order to fulfill that requirement, specific ligands could be chosen to coordinate with the metallic cations in the deposition solution, forming complex ions, to prevent the metallic cations from directly reacting with the anions in the deposition solution. Then, by electrochemically oxidizing or reducing such protecting ligands on the electrode surface, the metallic ions are exposed and the following chemical reaction between the metallic cations and anions in the solution occurs. An example of this method is the electrodeposition of CuO triggered by the electrochemical oxidation of the tartrate ligand of the Cu(II)-tartrate complex in an alkaline solution [30]. When choosing the protecting ligands, the formation constant of the formed metallic complex, the affinity between the metallic cations and the targeted anions, and the equilibrium potential of the redox couple of the ligand need to be comprehensively considered.

2.2 Key Parameters for Epitaxial Electrodeposition

There are many adjustable experimental parameters for electrodeposition, which could affect different properties of the deposits simultaneously. For example, the deposition potential could affect the composition, morphology, grain size, and crystallographic orientation of the deposits [31-33], deposition current density could vary the nucleation density, morphology, growth rate, and adhesion of the deposits to the substrate, and deposition temperature could change the growth rate and crystallinity of the deposits. Besides, many additives in the deposition solution could be used to adjust the growth of the deposits along certain crystallographic orientations (resulting in different morphologies of the deposits) [28, 34] or regulate the electric field distribution on the substrate surface to promote the growth of the deposits at desired positions (e.g., for the electrodeposition of metal interconnects in the manufacture of integrated circuits). Moreover, many other experimental parameters, such as pH of the deposition solution, conductivity of the substrate, and mass transfer of the active species in the deposition solution could influence the electrodeposition in different ways. It is worth mentioning that the mechanisms and influencing factors for the electrodeposition of various materials could be different, which have been introduced in many books and discussed in the relevant literature [35-37]. In this review, we will focus on reviewing the key parameters that could affect the epitaxial growth of the electrode posited films.

2.2.1 Substrate

While common electrodeposition could be carried out on any conductive and semiconductive substrate, epitaxial electrodeposition is mostly performed on

sin gle-crys talline substrates, including conductive metal single crystals (e.g., Au, Ni, and Cu) and semiconductor single crystals (e.g., Si, InP, and GaN). To date, various functional materials have been epitaxially electrodeposited onto different single crystals, such as Fe_3O_4 [7, 38], Co_3O_4 [19], $Co_xFe_{3-x}O_4$ [8], ZnO [29, 39], Cu_2O[40] and CuO[41] on Au single crystals, Cu_2O[42] and CdTe[43] on InP single crystals, and Au[44, 45], Cu[46, 47], Ag[48], and Cu_2O[49] on Si single crystals. In most cases, these epitaxial films grow with thermodynamically controlled orientations that are determined by the free energy of formation of the films on the single-crystal surfaces[50]. Normally, the electrodeposited epitaxial films tend to grow with crystallographic orientations that minimize the lattice mismatch between the deposited film and the single crystal surface, which could be calculated by using the following equation,

$$\text{Lattice mismatch} = (d_{\text{film}} - d_{\text{substrate}})/d_{\text{substrate}} \quad (13)$$

where d is the lattice spacing of the crystal planes parallel to the substrate surface. Generally, it is ideal for the epitaxial growth of the electrodeposited materials when the lattice mismatch is less than 5%. Epitaxial electrodeposition could still be achieved by forming a semi-coherent interface when the lattice mismatch ranges from 5% to 25%. When the lattice mismatch is even larger, epitaxy could possibly be achieved by in-plane rotation of the electrodeposited film and/or formation of coincidence lattices, which could reduce the lattice mismatch to facilitate the epitaxial growth[51, 52]. For example, the lattice mismatch between Ni(111) substrate and Fe_3O_4 could be dramatically reduced from +138 % to -0.7% by forming a coincidence, in which 5 unit meshes of O coincide with 12 unit meshes of Ni in the <011> directions (as shown in Figure 1a)[52]. Cu(100) film could be epitaxially electrodeposited on Si(100) single-crystalline wafer through a 45° in-plane rotation of the Cu film with respect to the Si substrate[46].

In addition to the lattice mismatch, the chemical stability of the substrate needs to be considered while performing epitaxial electrodeposition. Despite their high costs, single crystals of noble metals are preferred substrates for epitaxial electrodeposition due to their great conductivity and excellent chemical inertness. Non-precious metal substrates such as Ni and Cu single crystals might not be stable in some deposition systems. For instance, the single-crystalline Ni substrate might not be suitable for epitaxial electrodeposition in acidic deposition solutions due to its dissolution in acids. In contrast to the electrodeposition on conductive metal substrates, the electrodeposition on semiconductors is more complicated. First, the rectifying property of semiconductors needs to be considered if used as the substrates for electrodeposition. Second, the complexity of the semiconductor-solution interfaces results in more challenges in epitaxial electrodeposition on semiconductors. Take the most used single-crystalline semi-conductor substrate, single-crystal Si, as an example, it is challenging to epitaxially electrodeposit metal on H-terminated Si because of the propensity of Si to form a surface oxide layer in aqueous electrolytes (examples will be given in Section 2.2.2). Therefore, a sufficiently negative potential is usually applied before inserting the Si substrate into the electrolyte to avoid the formation of amorphous SiO_x layers. This process is known as prepolarization[53].

2.2.2 Mode and Magnitude of Electrical Stimulation

Like any common electrodeposition, the electrodeposition of epitaxial films is also initiated by imposing an electrical stimulation, i.e., applying an electrical potential/current to the substrate. Thus, the electrical stimulation is unquestionably an important parameter for epitaxial electrodeposition. Epitaxial electrodeposition could be carried out with different modes of electrical stimulation and the most common ones are potentiostatic (i.e., constant potential), galvanostatic (i.e., constant current), and pulsed potential/current modes, which could be controlled by the programmed sequences integrated into an electrochemical workstation. Potentiostatic or galvanostatic electrodeposition is usually used to produce epitaxial films with a uniform composition, whereas pulsed potential/current electrodeposition can produce compositionally modulated epitaxial layers, such as epi-

taxial superlattices (more detailed introduction on epi taxial superlattices will be presented in Section 4.2.2).

The magnitude of the applied potential/current could affect the epitaxial growth of the deposits. As mentioned in Section 2.2.1, in many cases the crystallographic orientations of the deposited films follow the orientation of the single-crystal substrate (i.e., the thermodynamically controlled orientation). However, such an epitaxial relationship between the electrodeposited epitaxial film and the single-crystal substrate might be overturned when the applied deposition potential results in an overpotential larger than a threshold value, at which the growth orientations of the deposited films are switched to kinetically preferred orientations[50]. For example, the electrodeposited Cu_2O film follows a [100] out-of-plane orientation of the Au(100) substrate at a low overpotential but switches to a kinetically preferred [110] out-of-plane orientation at a threshold overpotential of -118 mV. This abrupt change of growth orientation of the deposits is triggered by the coalescence of three-dimensional islands on single-crystal substrates. Such a transformation from the thermodynamically controlled growth orientation to the kinetically preferred growth orientation could also be achieved by controlling the magnitude of the applied current, where low current densities result in thermodynamically controlled orientations and high current densities lead to kinetically preferred orientations[54].

It is worth mentioning that it is not guaranteed to obtain epitaxial films by using low-overpotential electrodeposition. Sometimes, a more delicate maneuver on the applied potential is required in order to realize the epitaxial growth of the electrodeposited films. For example, the Cu film electrodeposited on Si(100) at a low overpotential (e.g., -0.5 V vs. Ag/AgCl) is polycrystalline due to the formation of a disordered SiO_x surface layer. In order to prevent the surface oxidation of the Si(100) single-crystal substrate, the electrodeposition of Cu is preferred to being carried out at a potential more negative than the potential where the Si substrate oxidizes. However, the Cu film electrodeposited at a high overpotential (e.g., -1.5 V vs. Ag/AgCl) is powdery with poor adhesion to the substrate, which is a typical phenomenon for metal electrodeposition at high overpotentials. To tackle this dilemma, Switzer group developed a two-step potentiostatic electrodeposition method to epitaxially grow Cu(100) film on n-Si(100). First, the epitaxial Cu seeds were nucleated during the initial 2 s pulse at -1.5 V vs. Ag/AgCl, at which the H-terminated Si surface was also protected from oxidation. Then, the epitaxial Cu seeds further grew and coalesced into an epitaxial Cu film at -0.5 V vs. Ag/AgCl (Figure 1b)[46].

The applied current density can influence the crystallinity of the deposits by affecting the deposition rate. Usually, lower current densities result in higher crystallinity of the epitaxial films, while too high current densities can even result in amorphous deposits. Therefore, the applied current density should be controlled within a certain range for the fabrication of epitaxial films by electrodeposition. Furthermore, the grain size of the deposits usually decreases with the increased current density due to higher nucleation densities endowed by the high applied current density. As shown in Figure 1c, the grain size and aspect ratio of the electrodeposited epitaxial films of Cu_2O decrease with the increased applied current density[42].

2.2.3 Parameters of Electrolyte

(i) Temperature

Epitaxial films are the films with well-defined growth orientations, which means that they possess relatively high crystallinity. Generally, the crystallinity of the deposit is a strong function of the temperature of the electrolyte. Elevated temperatures usually result in higher crystallinity for the deposits[19, 55]. For instance, amorphous Co_3O_4 with poor adhesion was produced when electrodeposited at a relatively low temperature of 50 ºC, and epitaxial films of Co_3O_4 with significantly improved crystallinity could be electrodeposited at a higher temperature of 103 ºC (Figure 1d). However, a too fast deposition rate endowed by a high deposition temperature might result in reduced uniformity and adhesion of the deposits. Besides, the

stability of the deposition solution generally decreases as the temperature increases[56]. Therefore, the electrolyte temperature should be carefully optimized for the epitaxial electrodeposition.

(ii) Ion Concentration

The concentrations of different species in the deposition solution typically have impacts on the mass transfer and current density. A high concentration of the active ions usually results in a higher current density (i.e., a higher rate of deposition) and faster mass transfer, which in turn affects the morphology, grain size, and adhesion of the deposit. Epitaxial electrodeposition is usually performed at low ion concentrations to achieve low deposition rates and improved the crystallinity of the deposits[19, 57].

(iii) pH

For the electrodeposition reactions involving H^+ and/or OH^- (such as the electrodeposition of metal oxides/hydroxides), the pH of the deposition solution might affect the epitaxial growth of the desired material by influencing the deposition potential. In addition, the pH of the deposition solution might affect the morphology and orientation of the metal films by the parasitic hydrogen evolution reaction (HER)[58, 59]. This is because the adsorbed H generated by the HER can affect metal nucleation on the substrate surface, or the generated H_2 bubbles will result in the stirring effect to affect the growth of the deposits. The pH of the deposition solution might also affect the selective adsorption of ions, thus resulting in different kinetically controlled orientations (usually are the slow-growing faces) and morphologies[60]. For example, the morphology of Cu_2O electrodeposited on InP (001) changes from nanopyramids with the <111> direction

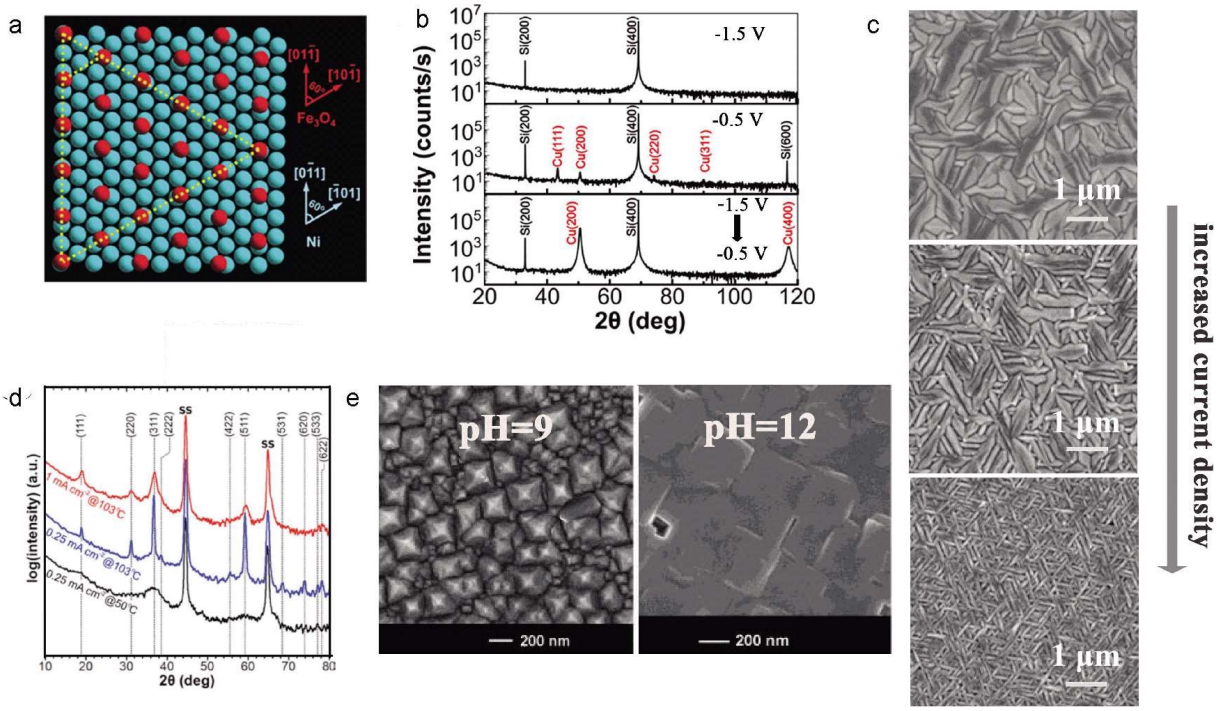

Figure 1 (a) Interface model for Fe_3O_4(111) on Ni(111). The light-blue spheres are Ni atoms and the red spheres are O atoms. Reproduced with permission of Ref.[52], copyright 2011 American Chemical Society. (b) XRD patterns of Cu films electrodeposited at -1.5 V for 1 h, -0.5 V for 10 min, and stepped from -1.5 V for 2 s to -0.5 V for 10 min. Reproduced with permission of Ref.[46], copyright 2018 American Chemical Society. (c) The morphology change of the Cu_2O films on InP(111) electrodeposited with increased current density. Reproduced with permission of Ref.[42], copyright 2005 American Chemical Society. (d) XRD patterns of Co_3O_4 electrodeposited at different temperatures (the blue and black curves) Reproduced with permission of Ref.[19], copyright 2012 American Chemical Society. (e) SEM images of Cu_2O electrodeposited at pH 9 and pH 12. Reproduced with permission of Ref.[61], copyright 2003 American Chemical Society.

at a pH of 9.0 to nanocubes with the <100> direction at a pH of 12.0 (Figure 1e)[61].

3 Characterizations of the Epitaxial Films

The electrodeposited films can be clarified into polycrystalline, textured, and epitaxial films. As shown in Figure 1a, epitaxial films are crystallographically oriented in both out-of-plane (i.e., perpendicular to the substrate surface) and in-plane (i.e., parallel with the substrate surface) orientations. In contrast, textured films are out-of-plane oriented but not in-plane oriented, and polycrystalline films are not oriented in either out-of-plane or in-plane orientation. Therefore, to determine whether the films are epitaxial, the out-of-plane and in-plane orientations of the films need to be characterized. In this section, common methods employed to characterize the epitaxial films are summarized.

3.1 X-Ray Diffraction

The out-of-plane orientation of the films could be determined by the XRD 2θ scans, in which only one family of planes is presented in the XRD 2θ scans for textured and epitaxial films. The in-plane orientation of the films could be detected by using the XRD pole figures. Pole figures are run by choosing a diffraction angle for a plane that is not parallel with the surface of the film. The tilt angle of the sample, χ, is then incrementally varied from 0 to 90°, with the azimuthal angle, ϕ, varied from 0 to 360° at each value of χ (Figure 2b)[44]. Peaks occur in the pole figure when the Bragg condition is satisfied. As shown in Figure 2c, the epitaxial films show "spot patterns", whereas textured and polycrystalline films usually show "ring patterns" and uniform background of diffraction, respectively.

3.2 Electron Backscatter Diffraction

When the deposited films are too thin, it is difficult to obtain information about the orientation by XRD due to the weak diffraction intensity of these films compared to the substrate. In this case, electron backscatter diffraction (EBSD), as an accessory for the scanning electron microscope, can be a useful

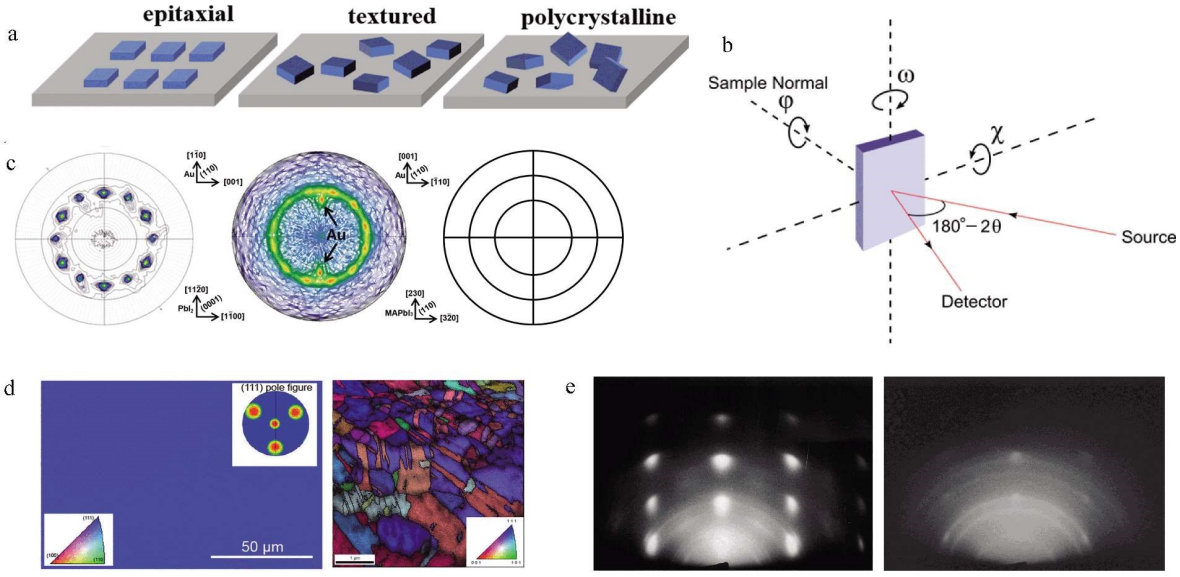

Figure 2 (a) Schematic illustration of the epitaxial, textured, and polycrystalline films. (b) X-ray measurement geometry for pole figures. Reproduced with permission of Ref.[45], copyright 2017 American Chemical Society. (c) XRD pole figures of epitaxial PbI_2 (left), textured $MAPbI_3$ (middle), and polycrystalline films. Reproduced with permission of Ref.[22], copyright 2015 American Chemical Society. (d) EBSD maps of Cu films on α-Al_2O_3 single crystal (left). Reproduced with permission of Ref.[66], copyright 2017 American Chemical Society. EBSD maps of polycrystalline Cu films (right). Reproduced with permission of Ref.[67], copyright 2007 American Institute of Physics. (e) RHEED patterns of CdS films with the best epitaxy (left) and inferior epitaxy (right). Reproduced with permission of Ref.[68], copyright 1997 Springer-Verlag.

tool to analyze the out-of-plane orientation of the films[62]. Compared to other characterization methods, EBSD has the advantages of simple sample preparation and rapid analysis. Single color will be present in EBSD inverse pole figure (IPF) map for the film with ordered out-of-plane orientation (as seen in Figure 2d).

3.3 *In-Situ* Scanning Tunneling Microscopy

In-situ scanning tunneling microscopy (*in-situ* STM) has been commonly used to investigate the initial stage of the underpotential deposition (UPD) of the epitaxial metal films. With the use of *in-situ* STM, real-time and high-resolution images of UPD process can be obtained, and the changes of the structure of the electrodeposited metal with electrode potential and time can be directly observed, thus allowing one to understand the interaction between the deposited metal and the substrate as well as the mechanism of nucleation and growth at the initial stage of electrodeposition. So far, Allongue[13] and Mao groups[63-65] have utilized *in-situ* STM to study the mechanism of UPD of various metals on single-crystal substrates.

3.4 Reflection High Energy Diffraction

Reflection high energy diffraction (RHEED) employs a high-energy electron beam (E = 5 ~ 100 keV) incident on the sample surface at a small grazing incidence angle to diffract the electron beam on the sample surface to obtain an electron diffraction pattern reflecting the structural information of the surface. RHEED is developed with the development of molecular beam epitaxy technology and is often used to monitor the growth process of thin films *in situ*. For epitaxial films, due to their single-crystalline properties, a series of well-aligned spots will be displayed on the electron diffraction pattern, while a series of concentric circles of different radii will be present for textured and polycrystalline films (as shown in Figure 2e).

4 Electrodeposited Functional Epitaxial Films for Electronics

The electronic properties of materials are usually improved as the structural order increases due to the minimization of the density of grain boundaries. In this section, we will review some electrodeposited epitaxial films of metals and semiconductors with certain electronic, electromagnetic, and photovoltaic properties, which could be applied or potentially applied for electronics.

4.1 Epitaxial Films of Metals

Epitaxial metal films are single-crystal-like metal films with specific in-plane and out-of-plane orientations. Due to the low cost and high controllability, epitaxial electrodeposition has been widely utilized to prepare various single-crystal-like metal films. The single-crystal-like metal films are a great alternative to bulk single crystals while used as substrates to grow epitaxial functional materials due to their much lower costs. In addition, epitaxial electrodeposition of metals has also attracted increasing attention recently in the metal anodes of rechargeable metal-based batteries. Furthermore, epitaxial electrodeposition of a ferromagnetic metal on single-crystalline conductive or semiconductive substrates is interested in electromagnetic applications such as spintronics.

4.1.1 Proxies for Single Crystals

Single-crystal-like metal films can serve as inexpensive alternative substrates to bulk single-crystal metals for epitaxial electrodeposition of grain boundary-free functional materials with improved performance. Single-crystal Si is an excellent substrate to electrodeposit single-crystal-like metal films because of its relatively low cost than other single-crystal substrates, high compatibility with many microfabrication techniques, and a flat surface on the atomic scale that can be prepared by a reproducible wet chemical etching[69]. As mentioned in Section 2.2.1, epitaxial electrodeposition of metals on Si is challenging due to the propensity of Si to be oxidized[46]. Therefore, the key to realizing the epitaxial electrodeposition of metal films on Si is to prevent the oxidation of Si. So far, epitaxial electrodeposition of single-crystal-like metal films of Au, Ag, and Cu on single-crystal Si has been reported.

Single-crystal Au is a commonly used substrate for epitaxial electrodeposition due to its chemical inertness, but it is very expensive. To obtain proxies for

Au single crystals, the direct electrodeposition of epitaxial Au films on Si has been widely investigated, which was pioneered by Allongue and coworkers, and further studied by Switzer et al. Allongue and coworkers investigated the electrochemical growth of Au on H-terminated Si(111) (H-Si(111)) surfaces from alkaline $KAu(CN)_2$ or acidic $HAuCl_4$ solutions[70-74]. Under the alkaline condition, a 3D island growth was observed, and the density of islands and the film structure were controlled by the deposition potential. In the acidic $HAuCl_4$ solution, atomically smooth epitaxial Au film was obtained by applying a very negative potential[71]. The Si wafer was prepolarized before immersing into the deposition solution to prevent the oxidation of Si. It was found that promoting a strong hydrogen evolution reaction (HER) in parallel with Au electrodeposition was essential to growing atomically flat Au(111) films on Si(111) due to the enhanced mobility of the Au adatoms from the Au islands to the Au/Si boundary[73]. The prepared epitaxial Au/Si (111) could serve as a nonmagnetic substrate for the epitaxial growth of ultrathin magnetic metals.

Switzer group electrodeposited nanometer-thick epitaxial layers of Au on Si(100), Si(110), and Si (111) to serve as proxies for bulk single-crystal Au[44]. Even though there is a -24.9% lattice mismatch between the electrodeposited Au film and the Si substrate, smooth epitaxial Au films could be produced by the formation of coincident site lattices (CSLs), which results in a lower lattice mismatch of +0.13%. The prepared Au/Si substrates are cheap and highly ordered for the electrodeposition of other epitaxial films such as Cu_2O, which is well-oriented in both out-of-plane and in-plane orientations (as shown in Figure 3a-b).

Once the electrodeposited epitaxial metal films are lift-off from substrates, free-standing single-crystal-like metal foils can be obtained. As shown in Figure 3c, light irradiation was introduced to generate holes at the Au/n-Si interface to grow a sacrificial SiO_x layer which was then etched by 5% HF to detach the electrodeposited epitaxial Au foil from the Si substrate[45]. The prepared single-crystal-like Au foils are flexible and optically transparent, which makes them potentially used in the fabrication of flexible and wearable displays, solar cells, and sensors. As expected, epitaxial Cu_2O films electrodeposited on the single-crystal-like Au foils show a lower value of diode quality factor (n) than the polycrystalline counterparts deposited on stainless steel (Figure 3d and e).

Ag epitaxially electrodeposited on Si is also attractive due to its lower cost than Au. Nanometer-thick epitaxial Ag films were electrodeposited onto single-crystal Si by applying a very negative pre-polarization and growth potential[48]. The epitaxy of the Ag films is dependent on not only the substrate but also the deposition solution. The Ag films electrodeposited from the acetate bath follow the out-of-plane and in-plane orientations of Si(111), Si(110), and Si(100) wafers, whereas the Ag films electrodeposited from the cyanide bath grow epitaxially only on Si(111) wafers.

When a chiral surface is used as the substrate, it is possible to produce chiral metal surfaces by epitaxial electrodeposition. The (643) surface of face-centered-cubic (fcc) metals such as Au, Ag, Pt, and Cu is chiral due to the lack of mirror symmetry. Switzer group demonstrated that chiral Au surfaces could be produced by epitaxial electrodeposition of Au onto commercially available Si(643) wafers[53]. These Au-coated Si wafers could then serve as substrates to epitaxially electrodeposit other metals such as Pt, Ni, Cu, and Ag to produce more active chiral surfaces. This work provides a pathway for producing chiral surfaces of a wide range of materials by epitaxial electrodeposition.

Compared with noble metals Au and Ag, Cu is more earth-abundant and cheaper, so the preparation of single-crystal-like Cu films by electrodeposition has also been investigated. The electrodeposition of Cu on H-Si(111) from alkaline CuCN solutions was first investigated by Allongue group[75]. Careful control of the deposition potential led to different electronic properties of the n-Si/Cu junctions such as perfect n-Si/Cu Schottky diodes or ohmic contacts. The electrodeposition of epitaxial films of Cu on Si single crystals was further investigated by Switzer's group[46, 47]. As discussed in Section 2.2.2, epitaxial Cu(100)

films could be produced by a two-step potential electrodeposition on Si(100) (as shown in Figure 3f). The mismatch between the lattices of Cu(100) and Si(100) reduces from -33.43% to -5.86% by rotating in-plane by 45°. In addition, the formation of a SiO_x interlayer between Cu and Si during deposition allowed for a simple epitaxial lift-off of the Cu film to produce flexible single-crystal-like Cu foils (as shown in Figure 3g). Epitaxial Cu films could also be electrodeposited on the self-assembled monolayer (SAM) of the amino acid L-cysteine on Au(111)[47]. A coordination-controlled deposition mechanism was proposed in which the nucleation and growth of Cu are on the top of SAMs via electrochemical reduction of Cu^{2+} ions coordinated to the SAM (Figure 3h). Benefiting from the presence of the SAM, epitaxial Cu films could be directly lift-off without etching, producing flexible single-crystal-like Cu(111) foils. This research opens interesting new avenues for epitaxial electrodeposition on functional SAM templates.

4.1.2 Highly Reversible Anodes for Metal-Based Batteries

Epitaxial metal electrodeposition has recently been found to be important for highly reversible anodes in

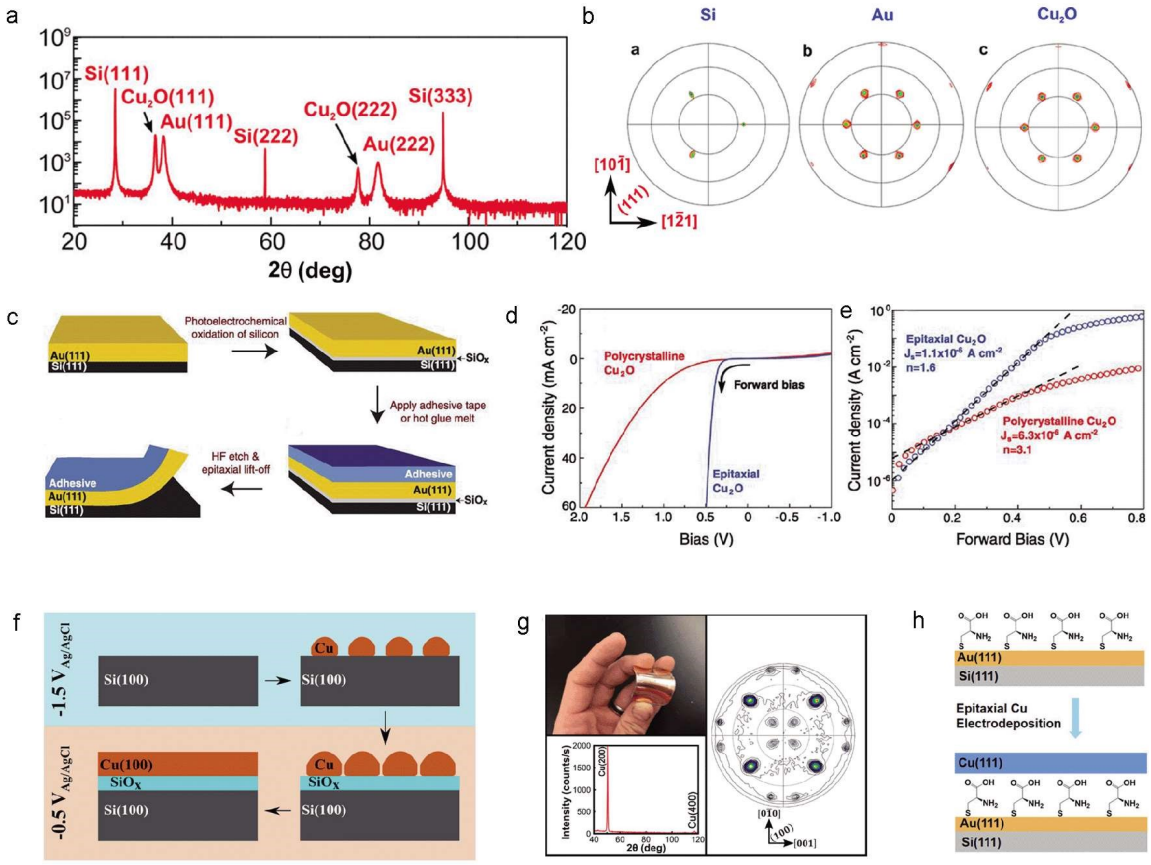

Figure 3 (a) XRD 2θ scan and (b) pole figures of the electrodeposited Au and Cu_2O on Si(111). Reproduced with permission of Ref.[44], copyright 2016 American Chemical Society. (c) Schematic illustration for epitaxial lift-off of an electrodeposited epitaxial Au foil on Si(111). (d) Current-voltage response of Cu_2O diode on the epitaxial Au foil and polycrystalline stainless steel substrates. (e) Dark saturation current density (J_s) and diode quality factor (n) of the epitaxial and polycrystalline Cu_2O diodes[45]. Reproduced with permission of Ref.[45], copyright 2017 The American Association for the Advancement of Science. (f) Mechanistic illustration of epitaxial electrodeposition of Cu on Si(100), and (g) Optical image, XRD 2θ scan, and pole figure of the electrodeposited epitaxial Cu foil lift-off from the Si(100) substrate. Reproduced with permission of Ref.[46], copyright 2018 American Chemical Society. (h) Schematic illustration of epitaxial electrodeposition of Cu(111) on an L-cysteine SAM on Au(111)/Si(111). Reproduced with permission of Ref.[47], copyright 2020 American Chemical Society.

rechargeable metal-based batteries. The dendrite-free Li anode formed by epitaxial electrodeposition was realized by cycling in the electrolyte containing LiBr and $LiNO_3$ under O_2 atmosphere[76]. This dendrite-free morphology of Li originated from the formation of an ultrathin and homogeneous Li_2O-rich solid-electrolyte interface layer during the discharge process, in which the native incompact passivation layer was removed by Br^- and the freshly formed Li surface was passivated by NO_3^- (as shown in Figure 4a). The symmetrical Li|Li cell cycled with epitaxial Li anode exhibited a lower voltage increase, which indicated improved stability of the Li anode. Zheng et al. designed the epitaxial electrodeposition of Zn on the surface of graphene with a low lattice mismatch to Zn[77]. As shown in Figure 4b and c, compared to that grown on the polycrystalline surface of stainless steel, the Zn platelets electrodeposited on graphene are well-directed and are parallel to the graphene substrate, which could greatly avoid the formation of dendrites during battery cycling. The epitaxial Zn anode shows excellent reversibility over thousands of cycles (Figure 4d). This work demonstrates that epitaxial electrodeposition can serve as a simple and efficient method to inhibit the formations of metal dendrites, which undoubtedly accelerates the development of metal-based batteries[78].

4.1.3 Ultrathin Ferromagnetic Films

Electrodeposition of ultrathin ferromagnetic films has aroused much attention due to the observed giant magnetoresistance (GMR) and perpendicular magnetization anisotropy (PMA), which are of interest for high-density data storage and spintronic devices[79]. PMA in ultrathin films is related to specific crystallographic structures and orientations. It is thus necessary to prepare epitaxial ultrathin ferromagnetic films.

Electrodeposition and magnetic characterizations of epitaxial ferromagnetic metal films on Au(111) have been studied by Allongue group. The epitaxial films of Co, Ni, and Fe could be electrodeposited on Au(111) from the corresponding metal sulfate solutions[80]. The growth mode of these metals is strongly related to the deposition potential[81] and the anion of the deposition solution[82]. For the Fe/Au(111) system,

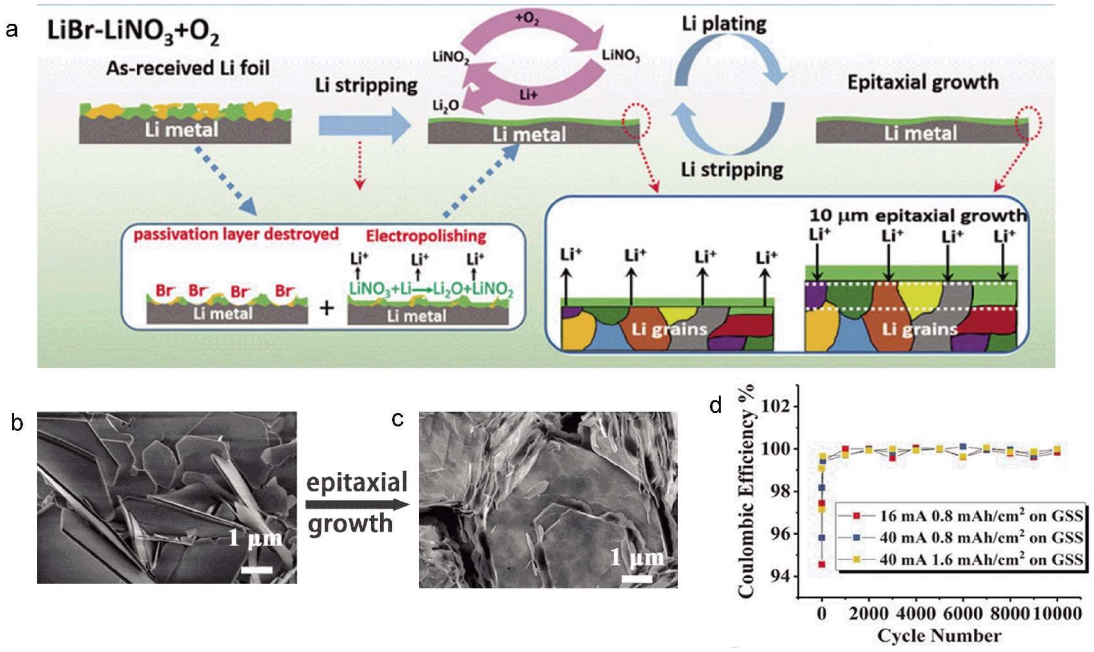

Figure 4 (a) Schematic of the Li stripping/planting in the electrolyte containing LiBr-$LiNO_3$ under O_2 atmosphere. Reproduced with permission of Ref.[76], copyright 2018 Wiley-VCH. SEM images of Zn deposited on (b) stainless steel and (c) graphene-coated stainless steel. (d) Coulombic efficiency of epitaxial Zn anodes. Reproduced with permission of Ref.[77], copyright 2019 The American Association for the Advancement of Science.

the Fe film undergoes a structural transition from the fcc-Fe(111) to bcc-Fe(110) when the film is thicker than 2-3 monolayers (ML)[83]. For the Co/Au(111) system, when the potential is more negative than -1.2 V vs. mercurous sulfate electrode (MSE), the electrodeposition of Co on Au(111) transits from a 3D to 2D growth mode. In addition, the growth is in a 2D mode in the Cl^- solution but a 3D mode in the SCN^- solution. The PMA of the deposited metal films is also greatly influenced by the thickness of the films[6] and the pH of the solution[84].

High-quality epitaxial metal films could also be produced by electrochemically reducing the pre-electrodeposited epitaxial metal oxide films. For example, Switzer and He have reported that epitaxial Fe[85] and Bi[86] thin films could be produced by direct electrochemical reduction of pre-electrodeposited epitaxial Fe_3O_4 and δ-Bi_2O_3 thin films on Au single crystals, respectively. This work demonstrates the feasibility of solid-state epitaxial transformation of metal oxide films to the corresponding metal films and could be applied to produce special epitaxial metal/metal oxide heterojunctions as well as different kinds of epitaxial alloy films from the corresponding mixed metal oxides.

Epitaxial electrodeposition of ferromagnetic metal films onto semiconductor substrates is also attractive due to the efficient injection of spin-polarized electrons into semiconductors for spintronic applications. The Fe/GaAs interface is of interest due to its magnetic properties and the small lattice mismatch (1.4%) between Fe(001) and GaAs(001). The Fe/GaAs interfaces fabricated by molecular-beam epitaxy usually show interfacial ternary phases ($Fe_3Ga_{2-x}As_x$) due to interdiffusion[87]. In contrast, an abrupt Fe/GaAs interface could be obtained by electrodeposition of epitaxial Fe(001), Fe(111), and Fe(011) films on single-crystal n-type GaAs from ferrous ammonium sulphate electrolytes[88]. The presence of ammonia in the electrolyte has been shown to be crucial for the epitaxial growth of Fe on n-type GaAs because ammonia could coordinate with Fe^{2+} ions in solution to inhibit the formation of Fe oxides and aid in the Fe epitaxial alignment.

4.2 Epitaxial Films of Semiconductors

Semiconductors possess diverse optical and electrical properties, and are generally the key components of various optical and electrical devices. Compared to polycrystalline semiconductors, epitaxial semiconductor films are more attractive due to their improved optical and electrical properties and better device efficiencies. Therefore, the preparation of epitaxial semiconductor films by simple and inexpensive electrodeposition has been extensively investigated. In this section, the electrodeposited epitaxial films of metal oxides, chalcogenides, and metal halides will be covered.

4.2.1 Epitaxial Metal Oxide Films

Metal oxides show diverse functionality among inorganic materials[89]. Nanostructured metal oxides usually exhibit special optical and electronic properties which make them important components for various electronics. In this section, epitaxial thin films of some representative metal oxides fabricated by electrodeposition will be discussed.

ZnO is a large bandgap (3.3 ~ 3.6 eV) n-type semiconductor which is of interest for high-frequency piezoelectric resonators, conducting transparent windows for photovoltaic cells, and UV light-emitting devices. Epitaxial ZnO films could be electrodeposited onto single-crystal gallium nitride (GaN) by reduction of dissolved oxygen in an aqueous solution of $ZnCl_2$[90, 91]. The electrodeposition could be described by the following equation (Eq. 13).

$$Zn^{2+} + 0.5O_2 + 2e^- \rightarrow ZnO \quad (13)$$

The morphology of the deposited ZnO could be tailored from epitaxial dots to fully covering flat single-crystal-like films by grain merging after a long enough polarization time. The bandgap and photoluminescence of the deposited ZnO are affected by the applied potential and solution composition. Epitaxial growth of ZnO nanopillars with highly ordered out-of-plane and in-plane orientations has also been realized by electrodeposition on single-crystal Au substrates[39]. In addition, as an amphoteric oxide, ZnO could be electrodeposited from strongly alkaline so-

lutions by electrochemically lowering the local pH at the electrode surface[29]. The electrodeposition involves the production of H^+ through the electrochemical oxidation of ascorbate dianions as mentioned in Section 2.1. The obtained epitaxial ZnO films have a columnar structure and an epitaxial relationship of ZnO(0001)[10$\bar{1}$1]//Au(111)[1$\bar{1}$0] with the Au(111) substrate.

CuO with a narrow bandgap in the range of 1.2 ~ 1.5 eV can absorb light throughout the visible spectrum, which can be used in electrochromic devices[92]. Epitaxial films of CuO could be anodically electrodeposited on Au(100) from an alkaline solution of Cu^{2+}-tartrate at room temperature[93]. Particularly, the deposition mechanism of CuO involves the oxidation of the tartrate ligands of the Cu^{2+}-tartrate complex rather than the redox reaction of Cu^{2+} ions. If L- or D-tartaric acid instead of DL-tartaric acid was used in the deposition solution, the deposited epitaxial CuO films on Au(100) could show chirality[93]. That is, the CuO film ((S)-CuO) deposited from a solution of Cu^{2+}-(S,S)-tartrate has a strong [1$\bar{1}\bar{1}$] orientation, whereas the CuO film ((R)-CuO) shows a strong [$\bar{1}\bar{1}$1] orientation when deposited from a solution of Cu^{2+}-(R,R)-tartrate (Figure 5a). These electrodeposited chiral CuO films show specific selectivity toward the oxidation of enantiomeric tartrates. As shown in Figure 5b, (S)-CuO shows a higher activity toward the oxidation of (S, S)-tartrate and (R)-CuO shows a higher activity toward the oxidation of (R, R)-tartrate. In contrast, CuO deposited from a mixture of (S, S)- and (R, R)-tartrate shows no selectivity on tartrate oxidation. This result suggests that the chirality of the deposited CuO film is determined by the chirality of the tartrate ions in the deposition solution. This enantiospecific electrodeposition of CuO could also be achieved on Cu(111)[41] and Cu(110)[94] surfaces or by the use of other chiral complexes such as amino acids (alanine and valine[95]) and malic acid[96].

The high optical/UV absorption coefficiency of Cu_2O (with a bandgap of 2.17 eV) makes it a good light-harvesting material for solar cells[97]. Epitaxial films of Cu_2O have been produced by electrodeposition on (100) surfaces of Au[40], Si[49], and InP[98] from an alkaline Cu^{2+}-lactate solution. Morphologies of the electrodeposited Cu_2O were significantly affected by the substrate (Figure 5c). Different epitaxial relationships are observed between the deposited Cu_2O and the substrates, i.e., Cu_2O(001)[100]//Au(001)[100], Cu_2O(001)[100]//Si(001)[110], and Cu_2O(001)[100]//InP(001)[110]. Take the electrodeposition of Cu_2O on Si as an example, the Cu^{2+} is reduced to epitaxial Cu_2O seeds by the Si substrates in the initial electroless deposition, with the concomitant oxidation of Si to SiO_2. Then, the electrodeposition proceeds on the Cu_2O epitaxial seeds (Figure 5d). Epitaxial Cu_2O films usually show enhanced optoelectronic and photovoltaic properties, which is conducive to obtaining higher device efficiencies for Cu_2O-based diode and solar cells[99].

Many spinels, including Fe_3O_4 and some ferrites (i.e., mixed oxides composed of iron and another metal), could be produced by direct electrodeposition from aqueous solutions without any post-annealing process. Epitaxial electrodeposition of Fe_3O_4 on low-index planes of Au was realized initially from a solution of $(NH_4)_2Fe(SO_4)_2$[7, 38] and later from a more stable alkaline solution of Fe^{3+}-triethanolamine (TEA) complexes[18, 21, 52, 85]. In the case of electrodeposition from the alkaline solution, the phase of the electrodeposited film depends on the applied potential because the change of the applied potential would lead to the change of the concentration ratio of Fe^{2+}/Fe^{3+} ions on the electrode surface and possibly vary the mechanism of deposition. Specifically, Fe_3O_4 films were formed at relatively low overpotentials whereas ferrihydrite ($Fe_{10}O_{14}(OH)_2$) films were formed at relatively high overpotentials. The electrodeposited Fe_3O_4 films show a [111] out-of-plane orientation on Au(111) and Au(001), and a [110] out-of-plane orientation on Au(110). In addition to Fe_3O_4, Switzer and He have reported the electrodeposition of $Co_xFe_{3-x}O_4$[8], $Zn_xFe_{3-x}O_4$[100], $Ni_xFe_{3-x}O_4$[34] that could be used in magnetic or catalytic applications. The electrodeposition mechanism of these metal ferrites is analogous to the electrodeposition of Fe_3O_4, in which $Fe(TEA)^{3+}$ complex ions are

firstly electrochemically reduced into $Fe(TEA)^{2+}$ and the production of $Fe(TEA)^{2+}$ would trigger the deposition of $M_xFe_{3-x}O_4$ (M = Co, Zn or Ni) (Eqs. 14 and 15). Epitaxial $Co_xFe_{3-x}O_4$ films were electrodeposited on Au(111) from an alkaline $Fe(TEA)^{3+}$ and $Co(TEA)^{2+}$ solution[8]. The magnetic and electrical properties of the electrodeposited $Co_xFe_{3-x}O_4$ epitaxial films could be conveniently adjusted by controlling the Co:Fe ratio in $Co_xFe_{3-x}O_4$ through the deposition potential.

$$Fe(TEA)^{3+} + e^- \rightarrow Fe(TEA)^{2+} \quad (14)$$

$$2Fe(TEA)^{3+} + (1-x)Fe(TEA)^{2+} + xCo(TEA)^{2+} + 8OH^- \rightarrow Co^{2+}_xFe^{2+}_{1-x}Fe^{3+}_2O_4 + 3TEA + H_2O \quad (15)$$

4.2.2 Epitaxial Oxide Superlattices

Superlattices are periodically layered nanostructures with coherent stacking of atomic planes as shown in Figure 5e. Superlattices not only can maintain the properties of nanomaterials, but also are more conveniently integrated into electronic devices than conventional nanomaterials. Superlattices usually show enhanced mechanical properties, and unique optical and electronic properties compared to bulk materials, which have been widely applied for various photonics and electronics. For example, the GMR effect was first observed in Fe/Cr superlattices[101] and has been widely used in high-density data storage. Although superlattices have traditionally been produced by techniques such as molecular beam epitaxy, chemical vapor deposition, physical vapor deposition, and reactive magnetron sputtering, they could also be fabricated by electrodeposition. In addition to its cost-effectiveness, electrodeposition offers a unique advantage over other techniques by minimizing interdiffusion across interfaces because of the low processing temperatures.

Electrodeposition of superlattice is achieved by repeatedly pulsing the applied potential or current during the deposition (see in Figure 5f). Since different compositions are obtained at different deposition potentials or current densities, such pulse electrodeposition can yield the layer-by-layer superlattice structures. The thickness of each layer in the superlattices can be precisely controlled by adjusting the number of charges passed during each pulse (i.e., by controlling the current density and the dwell time of each pulse). The overall thickness of the superlattices is determined by the thickness of each bilayer (Λ in Figure 5e, also known as the modulation wavelength of superlattices) and the number of the bilayers (i.e., the cycle number of the pulse electrodeposition). The formation of superlattices could be verified by the observation of satellite peaks in the XRD 2θ scans (Figure 5g).

Switzer and co-workers have utilized electrodeposition to prepare various metal oxide superlattices. Usually, three criteria need to be satisfied for the successful electrodeposition of metal oxide superlattices[102]: i) the materials could be deposited as anhydrous oxides; ii) the composition of the deposit could be changed by varying the applied potential or current; iii) lattice mismatch of the layers A and B (Figure 5e) should be small to ensure that the material could be grown epitaxially. Epitaxial electrodeposition of Pb-Tl-O superlattices[102] on Au(100) was achieved by periodically pulsing anodic current between 0.05 and 5 $mA \cdot cm^{-2}$ at room temperature from an alkaline solution of $TlNO_3$ and $Pb(NO_3)_2$. The deposited layer is Tl-rich at the low current density and Pb-rich at the high current density. Fe_3O_4 superlattices could be produced by controlling the concentration ratio of Fe^{2+}/Fe^{3+} at the electrode surface through the applied potential[100]. Layers deposited at potentials more positive than -1.06 $V_{Ag/AgCl}$ have excessive Fe^{3+}, while those deposited at potentials more negative than -1.06 $V_{Ag/AgCl}$ have excessive Fe^{2+}. Therefore, stoichiometric Fe_3O_4 superlattices could be produced by pulsing the potential between -1.01 and -1.065 $V_{Ag/AgCl}$ in the $Fe(TEA)^{3+}$ deposition bath. In addition to stoichiometric superlattices, compositional superlattices in the $Fe_3O_4/ZnFe_2O_4$ system could also be electrodeposited from the same $Fe(TEA)^{3+}$ deposition bath with the addition of 30 $mmol \cdot L^{-1}$ Zn(II) by pulsing the potentials between -0.99 and -1.05 $V_{Ag/AgCl}$. Compositional superlattices in the $Co_xFe_{3-x}O_4$ system[8] were electrodeposited in a similar way, which was composed of alternately deposit-

ed $Co_xFe_{3-x}O_4$ epitaxial layers with two different Co: Fe ratios. As shown in Figure 5h, the electrodeposited $Co_xFe_{3-x}O_4$ superlattices show abrupt resistance switching phenomena with the changing of the external electric field, which could be potentially used in resistive random access memories (RRAMs).

4.2.3 Epitaxial Metal Chalcogenides Films

Metal chalcogenides are promising candidates for various electronics due to their unique physical and chemical properties. For example, many lead chalcogenides, such as PbS, PbSe, and PbTe, are narrow bandgap semiconductors, which can be utilized for laser diodes[103] and infrared detectors[104]. Epitaxial films of PbS could be obtained by cathodic electrodeposition on Au(100) from an acidic solution of $[Pb(S_2O_3)_2]^{2-}$ with an excess of $S_2O_3^{2-}$[105]. In an acidic solution, $S_2O_3^{2-}$ would spontaneously disproportionate to form colloidal sulfur (Eq. 16), which was adsorbed on the surface of the Au substrate. The epitaxial electrodeposition of PbS films on Au(100) was triggered by electrochemical reduction of $[Pb(S_2O_3)_2]^{2-}$ to Pb (Eq. 17), which might then react with the adsorbed S to form PbS.

$$S_2O_3^{2-} + 2H^+ \rightarrow S_{colloidal} + SO_2 + H_2O \quad (16)$$

$$[Pb(S_2O_3)_2]^{2-} + 2e^- \rightarrow Pb + S_2O_3^{2-} \quad (17)$$

Froment group reported the epitaxial electrodeposition of PbSe[106] and PbTe[107] on InP single crystals from solutions containing Pb^{2+} and Cd^{2+}. For the epitaxial electrodeposition of PbSe on InP(111), the presence of Cd^{2+} in the deposition solution is a prerequisite for the epitaxial growth because of the inhibition of dendritic growth of PbSe by Cd^{2+}. The epitaxy of the PbSe films was also influenced by the concentration of Cd^{2+} in the electrolyte and the best epitaxy could be achieved at a Cd^{2+} concentration of around 0.5 mol·L^{-1}. However, the electrodeposition

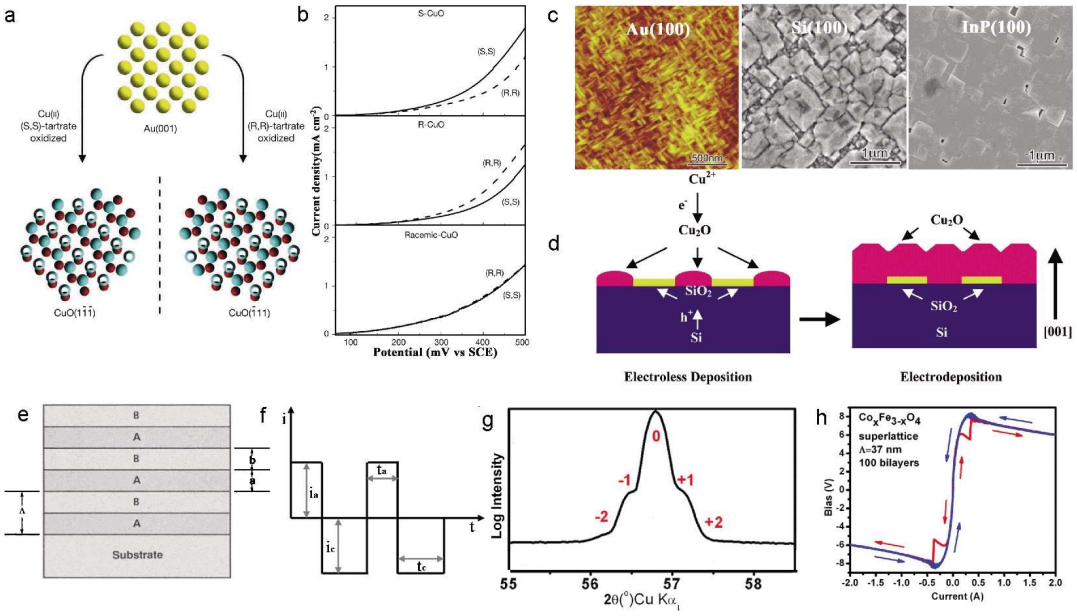

Figure 5 (a) Schematic illustration of enantiospecific electrodeposition of CuO on Au(100). (b) Chirality recognition of electrodeposited CuO by enantioselective oxidation of tartrates. Reproduced with permission of Ref.[93], copyright 2003 Springer Nature. (c) SEM images of Cu_2O layers electrodeposited on single-crystal Au(100), Si(100), and InP(100) substrates. Reproduced with permission of Ref.[98], copyright 2005 Wiley-VCH. (d) Illustration of the mechanism for the epitaxial electrodeposition of Cu_2O on Si(100). Reproduced with permission of Ref.[49], copyright 2002 American Chemical Society. (e) Ideal superlattice structure with square-wave modulation of composition or structure, or both. Reproduced with permission of Ref.[102], copyright 1990 The American Association for the Advancement of Science. (f) Scheme of pulse electrodeposition for superlattices. (g) Satellite peak observed in the XRD pattern of electrodeposited $Co_xFe_{3-x}O_4$ superlattices. (h) Resistance switching of electrodeposited $Co_xFe_{3-x}O_4$ superlattices. Reproduced with permission of Ref.[8], copyright 2012 American Chemical Society.

of PbSe on InP(100) exhibited a poor epitaxy because of weak adsorption of Cd^{2+} on InP (100). For the elec trodeposition of PbTe on InP(111), poor epitaxy was observed due to the large lattice mismatch between PbTe and InP(111).

SnS is a p-type semiconductor with a layered structure and its bandgap is ranging from 1.0 to 1.5 eV, which makes it potentially an efficient light-absorbing material for solar cells. SnS nanodisks with a high aspect ratio could be epitaxially electrodeposited onto Au(100) from an acidic solution of Sn^{2+}-tartrate complexes[108]. The electrodeposition of SnS was achieved by reduction of S in the presence of Sn^{2+}[109]. The electrodeposited SnS showed two different out-of-plane orientations of (100) and (301).

4.2.4 Epitaxial Metal Halide Films

Epitaxial metal halide semiconductors can serve as efficient carrier transport layers or light-absorbing layers, which are highly desired for photovoltaic cells due to the lower trap densities, longer diffusion lengths, enhanced photoluminescence, and higher conversion efficiencies compared to the polycrystalline ones[110, 111].

Highly ordered films of methylammonium lead iodide ($MAPbI_3$) perovskite could be produced by the conversion of electrodeposited epitaxial films of PbI_2[22] or PbO_2[9]. PbI_2 was electrodeposited on single-crystal Au substrates by electrochemically reducing molecular iodine to iodide ions with the presence of Pb^{2+} ions in the deposition solution. Strongly textured $MAPbI_3$ films were then produced by a vapor-assisted conversion from the epitaxial PbI_2 films. Epitaxial films of PbO_2 could be obtained by anodic electrodeposition on Au(100) and Au(111) from an alkaline solution of 0.1 mol·L^{-1} $Pb(NO_3)_2$[9, 54]. The epitaxial relationships between the electrodeposited PbO_2 and Au substrates were $PbO_2(100)[001]//Au(100)\langle 011\rangle$ and $PbO_2(100)[001]//Au(111)\langle 2\bar{1}\bar{1}\rangle$. As shown in Figure 6a-b, after immersing in a 2-propanol solution of CH_3NH_3I, the electrodeposited PbO_2 could be converted into epitaxial $MAPbI_3$ films with a well-oriented morphology. The orientation of the converted $MAPbI_3$ films was determined by the temperature of the conversion solution. Specifically, films converted at low temperatures have predominately a [001] orientation, whereas films converted at high temperatures have predominately a [110] orientation. The epitaxial films of $MAPbI_3$ show lower trap densities and higher photoluminescence intensities than their polycrystalline counterparts (Figure 6c-d).

Bi-based perovskite films are promising alternatives to the toxic Pb-based perovskites, which could be obtained by the conversion of Bi-containing precursors such as BiI_3. With the same trigger (i.e., reduction of molecular iodine to iodide in the presence of metal cations), the epitaxial films of BiI_3 with a high degree of in-plane and out-of-plane order could be electrodeposited on inexpensive Au(111)|Si(111) substrates[23]. These BiI_3 epitaxial films formed from the van der Waals layered material BiI_3 could be peeled off to produce single-crystal-like and free-standing BiI_3 foils. The epitaxial BiI_3 films could be further converted into $(CH_3NH_3)_3Bi_2I_9$ ($(MA)_3Bi_2I_9$) by topotactic transformation, which is a good solar light-absorbing layer for solar cells. As shown in Figure 6e-f, the converted $(MA)_3Bi_2I_9$ films are both out-of-plane and in-plane oriented. The epitaxial relationship between the $(MA)_3Bi_2I_9$ and Au(111) substrate is $(MA)_3Bi_2I_9(0001)[\bar{1}\bar{1}00]//Au(111)[\bar{1}\bar{1}0]$.

Due to the large room-temperature exciton binding energy (62 meV), high hole mobility (43.9 $cm^2\cdot V^{-1}\cdot s^{-1}$), and large bandgap (3.1 eV), CuI has shown to be a promising candidate in optoelectronics. Epitaxial CuI films could be electrodeposited on n-Si(111) by reducing Cu(II)-EDTA to Cu(I) in the presence of iodide[112]. For the deposition of CuI on Si, epitaxial CuI seed crystals are firstly nucleated on the freshly etched n-Si(111) surface, followed by the simultaneous oxidation of Si to form a thin layer of SiO_x and the lateral overgrowth of the CuI seeds into a continuous film. The presence of the SiO_x interlayer affords the chemical etch and lift-off of the deposits to produce highly textured CuI(111) foils.

CuSCN is an earth-abundant and wide bandgap (3.7 ~ 3.9 eV) p-type metal pseudohalide semicon-

ductor, which can serve as an excellent hole transport material due to its exceptional optical transparency, chemical stability, and good hole transport properties[113]. Epitaxial electrodeposition of CuSCN nanorods on the Au(111)/Si(111) substrate has been achieved by electrochemically reducing Cu(II) in the presence of SCN^- ions[10]. The phase of CuSCN is a function of the Cu^{2+}/SCN^- ratio in the deposition bath. Typically, a pure rhombohedral phase is produced with higher SCN^- concentrations, whereas a mixture of rhombohedral and hexagonal phases is produced with lower SCN^- concentrations. In addition, a highly ordered free-standing CuSCN foil with high transmittance could be obtained by epitaxial lift-off following a triiodide etch of the thin Au substrate (Figure 6g). Diodes composed of the epitaxial CuSCN show a more significant rectifying behavior and possess a lower value of quality factor than that with polycrystalline CuSCN (Figure 6h and i).

5 Summary and Perspectives

In this review, the common synthetic routes for the electrodeposition of different functional materials and the key experimental parameters that could be used to regulate the epitaxial growth of the deposited films are summarized. In addition, the characterization techniques that are used to investigate the out-of-plane and in-plane orientations of the deposited films are briefly introduced. Furthermore, some representative functional epitaxial films fabricated by electrodeposition with special electric, electromagnetic, and photovoltaic properties that could be potentially used in electronics are reviewed.

Electrodeposition is superior to other synthetic methods in terms of its low-cost, simplicity, and environmental friendliness. It avoids the use of high-pressure and high-temperature conditions, which imposes

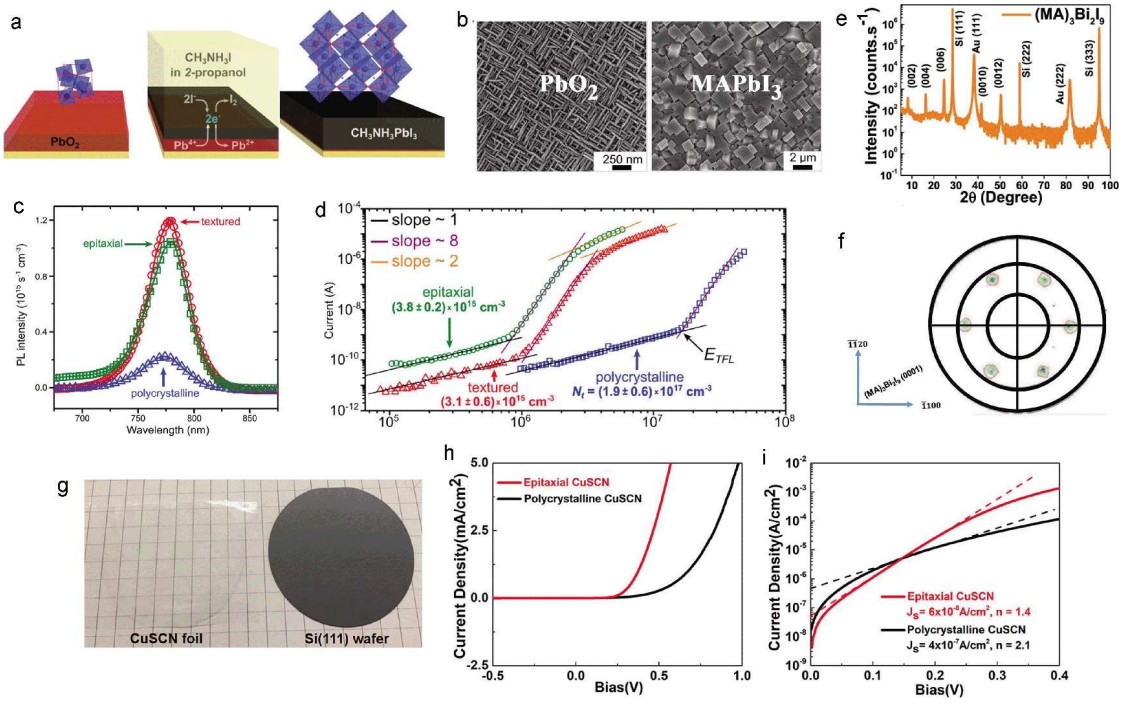

Figure 6 (a) Reaction scheme for the conversion of electrodeposited PbO_2 to $MAPbI_3$. (b) SEM images of PbO_2 and converted $MAPbI_3$. Comparisons of the PL intensity (c) and trap density (d) of epitaxial, textured, and polycrystalline $MAPbI_3$ films. Reproduced with permission of Ref.[9], copyright 2015 American Chemical Society. (e) XRD 2θ scan and (f) pole figure of the $(MA)_3Bi_2I_9$ film converted from epitaxial BiI_3 film. Reproduced with permission of Ref.[23], copyright 2020 American Chemical Society. (g) An electrodeposited epitaxial CuSCN foil (with a diameter of 2 inches) lift-off from the Si substrate. (h) Current-voltage (*J-V*) plot of Au/CuSCN/Ag diodes. (i) log(*J*)-V plot to measure the diode quality factor (n) and dark saturation current density (J_s). Reproduced with permission of Ref.[10], copyright 2022 American Chemical Society.

lower requirements on the equipment and thus leads to higher scalability. To date, a huge number of materials have been produced by electrodeposition. However, there are still many challenges for electrodeposition. Many adjustable parameters in electrodeposition are correlated, which sometimes causes difficulties in the optimization of the deposits. Besides, the electrodeposition in aqueous solutions is usually restricted in the potential window of water oxidation/reduction or significantly affected by the hydrogen/oxygen evolution reactions. Performing electrodeposition in ionic liquids instead of aqueous solutions is one of the ways to break through such limitations, but it usually leads to a higher cost and means a completely different design of experiments. Furthermore, it is still challenging to obtain the high-purity single-phase deposit by electrodeposition due to the complexity of the deposition solution and the possibly undetected side-reactions during the deposition. Better understandings on the deposition mechanisms and novel designs of the synthetic routes are desired to conquer these challenges.

Acknowledgments:

This work was supported by the Natural Science Foundation of Hunan Province (Grant No. 2021JJ30790), the National Natural Science Foundation of China (Grant No. 51972345), the Hunan Provincial Science and Technology Plan Project (Grant Nos. 2018RS3008 and 2017TP1001), the Open Sharing Fund for the Large-scale Instruments and Equipments of Central South University, and Postgraduate Scientific Research Innovation Project of Hunan Province (Grant No. 2021zzts0524).

Refefrences:

[1] Kang D, Kim T W, Kubota S R, Cardiel A C, Cha H G, Choi K S. Electrochemical synthesis of photoelectrodes and catalysts for use in solar water splitting[J]. Chem. Rev., 2015, 115(23): 12839-12887.

[2] Switzer J A, Hodes G. Electrodeposition and chemical bath deposition of functional nanomaterials[J]. MRS Bull., 2010, 35(10): 743-752.

[3] Gusley R, Ezzat S, Coffey K R, West A C, Barmak K. Influence of the seed layer and electrolyte on the epitaxial electrodeposition of Co(0001) for the fabrication of single crystal interconnects[J]. J. Electrochem. Soc., 2020, 167(16): 162503.

[4] Choi K S, Jang H S, McShane C M, Read C G, Seabold J A. Electrochemical synthesis of inorganic polycrystalline electrodes with controlled architectures[J]. MRS Bull., 2010, 35(10): 753-760.

[5] Zhang Y H, An M Z, Yang P X, Zhang J Q. Recent advances in electroplating of through-hole copper interconnection[J]. Electrocatalysis, 2021, 12(6): 619-627.

[6] Gundel A, Devolder T, Chappert C, Schmidt J E, Cortes R, Allongue P. Electrodeposition of Fe/Au(111) ultrathin layers with perpendicular magnetic anisotropy[J]. Phys. B: Condens. Matter, 2004, 354(1-4): 282-285.

[7] Sorenson T A, Morton S A, Waddill G D, Switzer J A. Epitaxial electrodeposition of Fe_3O_4 thin films on the low-index planes of gold[J]. J. Am. Chem. Soc., 2002, 124 (25): 7604-7609.

[8] He Z, Koza J A, Mu G J, Miller A S, Bohannan E W, Switzer J A. Electrodeposition of $Co_xFe_{3-x}O_4$ epitaxial films and superlattices[J]. Chem. Mater., 2013, 25(2): 223-232.

[9] Koza J A, Hill J C, Demster A C, Switzer J A. Epitaxial electrodeposition of methylammonium lead Iodide perovskites[J]. Chem. Mater., 2016, 28(1): 399-405.

[10] Luo B, Banik A, Bohannan E W, Switzer J A. Epitaxial electrodeposition of hole transport CuSCN nanorods on Au(111) at the wafer scale and lift-off to produce flexible and transparent foils[J]. Chem. Mater., 2022, 34(3): 970-978.

[11] Yan Z H, Liu H H, Hao Z M, Yu M, Chen X, Chen J. Electrodeposition of (hydro)oxides for an oxygen evolution electrode[J]. Chem. Sci., 2020, 11(39): 10614-10625.

[12] Pu J, Shen Z H, Zhong C L, Zhou Q W, Liu J Y, Zhu J, Zhang H G. Electrodeposition technologies for Li-based batteries: New frontiers of energy storage[J]. Adv. Mater., 2019, 32(27): 1903808.

[13] Allongue P, Maroun F. Electrodeposited magnetic layers in the ultrathin limit[J]. MRS Bull., 2010, 35(10): 761-770.

[14] Hangarter C M, Liu Y, Pagonis D, Bertocci U, Moffat T P. Electrodeposition of ternary $Pt_{100-x-y}Co_xNi_y$ alloys[J]. J. Electrochem. Soc., 2014, 161(1): D31-D43.

[15] Herrick R D, Kaplan A S, Chinh B K, Shane M J, Sailor M J, Kavanagh K L, McCreey R L, Zhao J. Room-temperature electrosynthesis of carbonaceous fibers[J]. Adv. Mater., 1995, 7(4): 398-401.

[16] Mahenderkar N K, Liu Y C, Koza J A, Switzer J A. Electrodeposited germanium nanowires[J]. ACS Nano, 2014, 8(9): 9524-9530.

[17] Munisamy T, Bard A J. Electrodeposition of Si from organic solvents and studies related to initial stages of Si growth[J]. Electrochim. Acta, 2010, 55(11): 3797-3803.

[18] Kothari H M, Kulp E A, Limmer S J, Poizot P, Bohannan E W, Switzer J A. Electrochemical deposition and characterization of Fe_3O_4 films produced by the reduction of Fe(III)-triethanolamine[J]. J. Mater. Res., 2006, 21(1): 293-301.

[19] Koza J A, He Z, Miller A S, Switzer J A. Electrodeposition of crystalline Co_3O_4-A catalyst for the oxygen evolution reaction[J]. Chem. Mater., 2012, 24(18): 3567-3573.

[20] Koza J A, Schroen I P, Willmering M M, Switzer J A. Electrochemical synthesis and nonvolatile resistance switching of Mn_3O_4 thin films[J]. Chem. Mater., 2014, 26 (15): 4425-4432.

[21] Kulp E A, Kothari H M, Limmer S J, Yang J B, Gudavarthy R V, Bohannan E W, Switzer J A. Electrodeposition of epitaxial magnetite films and ferrihydrite nanoribbons on single-crystal gold[J]. Chem. Mater., 2009, 21(21): 5022-5031.

[22] Hill J C, Koza J A, Switzer J A. Electrodeposition of epitaxial lead Iodide and conversion to textured methylammonium lead Iodide perovskite[J]. ACS Appl. Mater. Interfaces, 2015, 7(47): 26012-26016.

[23] Banik A, Bohannan E W, Switzer J A. Epitaxial electrodeposition of BiI_3 and topotactic conversion to highly ordered solar light-absorbing perovskite $(CH_3NH_3)_3Bi_2I_9$[J]. Chem. Mater., 2020, 32(19): 8367-8372.

[24] Therese G H A, Kamath P V. Electrochemical synthesis of metal oxides and hydroxides[J]. Chem. Mater., 2000, 12(5): 1195-1204.

[25] Yan Z H, Sun H M, Chen X, Liu H H, Zhao Y R, Li H X, Xie W, Cheng F Y, Chen J. Anion insertion enhanced electrodeposition of robust metal hydroxide/oxide electrodes for oxygen evolution[J]. Nat. Commun., 2018, 9: 2373.

[26] Lv Y, Zhang Z A, Lai Y Q, Liu Y X. Electrodeposition of porous $Mg(OH)_2$ thin films composed of single-crystal nanosheets[J]. J. Electrochem. Soc., 2012, 159(4): D187-D189.

[27] Aghazadeh M, Dalvand S, Hosseinifard M. Facile electrochemical synthesis of uniform β-$Co(OH)_2$ nanoplates for high performance supercapacitors[J]. Ceram. Int., 2014, 40 (2): 3485-3493.

[28] Kulp E A, Switzer J A. Electrochemical biomineralization: The deposition of calcite with chiral morphologies [J]. J. Am. Chem. Soc., 2007, 129(49): 15120-15121.

[29] Limmer S J, Kulp E A, Switzer J A. Epitaxial electrodeposition of ZnO on Au(111) from alkaline solution: Exploiting amphoterism in Zn(II)[J]. Langmuir, 2006, 22 (25): 10535-10539.

[30] Poizot P, Hung C J, Nikiforov M P, Bohannan E W, Switzer J A. An electrochemical method for CuO thin film deposition from aqueous solution[J]. Electrochem. Solid-State Lett., 2003, 6(2): C21-C25.

[31] Han S, Liu S Q, Yin S J, Chen L, He Z. Electrodeposited Co-Doped Fe_3O_4 thin films as efficient catalysts for the oxygen evolution reaction[J]. Electrochim. Acta, 2016, 210: 942-949.

[32] Hssi A A, Atourki L, Abouabassi K, Elfanaoui A, Bouabid K, Ihall A, Benmokhtar S, Ouafi M. Growth and characterization of Cu_2O for solar cells applications[M]. USA: Amer Inst Physics, 2018.

[33] Siegfried M J, Choi K S. Directing the architecture of cuprous oxide crystals during electrochemical growth[J]. Angew. Chem. Int. Ed., 2005, 44(21): 3218-3223.

[34] Li D J, Liu S Q, Ye G Y, Zhu W W, Zhao K M, Luo M, He Z. One-step electrodeposition of $Ni_xFe_{3-x}O_4$/Ni hybrid nanosheet arrays as highly active and robust electrocatalysts for the oxygen evolution reaction[J]. Green Chem., 2020, 22(5): 1710-1719.

[35] Zhou S M. Electrodeposition of metals: Principles and methods[M]. Shanghai: Shanghai Scientific & Technical Publishers, 1987.

[36] Tu Z M, An M Z, Hu H L. Modern alloy electrodeposition theory and technology[M]. Beijing: National Defense Industry Press, 2016.

[37] Paunovic M, Schlesinger M. Fundamentals of electrochemical deposition[M]. USA: John Wiley & Sons, Inc., 2006.

[38] Nikiforov M P, Vertegel A, Shumsky M G, Switzer J A. Epitaxial electrodeposition of Fe_3O_4 on single-crystal Au (111)[J]. Adv. Mater., 2000, 12(18): 1351-1353.

[39] Liu R, Vertegel A A, Bohannan E W, Sorenson T A, Switzer J A. Epitaxial electrodeposition of zinc oxide nanopillars on single-crystal gold[J]. Chem. Mater., 2001, 13(2): 508-512.

[40] Bohannan E W, Shumsky M G, Switzer J A. Epitaxial electrodeposition of copper(I) oxide on single-crystal gold (100)[J]. Chem. Mater., 1999, 11(9): 2289-2291.

[41] Bohannan E W, Kothari H M, Nicic I M, Switzer J A. Enantiospecific electrodeposition of chiral CuO films on single-crystal Cu(111)[J]. J. Am. Chem. Soc., 2004, 126 (2): 488-489.

[42] Liu R, Kulp E A, Oba F, Bohannan E W, Ernst F, Switzer J A. Epitaxial electrodeposition of high-aspect-ratio Cu_2O

(110) nanostructures on InP(111)[J]. Chem. Mater., 2005, 17(4): 725-729.

[43] Lincot D, Kampmann A, Mokili B, Vedel J, Cortes R, Froment M. Epitaxial electrodeposition of CdTe films on InP from aqueous solutions: role of a chemically deposited CdS intermediate layer[J]. Appl. Phys. Lett., 1995, 67 (16): 2355-2357.

[44] Switzer J A, Hill J C, Mahenderkar N K, Liu Y C. Nanometer-thick gold on silicon as a proxy for single-crystal gold for the electrodeposition of epitaxial cuprous oxide thin films[J]. ACS Appl. Mater. Interfaces, 2016, 8(24): 15828-15837.

[45] Mahenderkar N K, Chen Q Z, Liu Y C, Duchild A R, Hofheins S, Chason E, Switzer J A. Epitaxial lift-off of electrodeposited single-crystal gold foils for flexible electronics[J]. Science, 2017, 355(6330): 1203-1206.

[46] Hull C M, Switzer J A. Electrodeposited epitaxial Cu(100) on Si(100) and lift-off of single crystal-like Cu(100) foils [J]. ACS Appl. Mater. Interfaces, 2018, 10(44): 38596-38602.

[47] Luo B, Banik A, Bohannan E W, Switzer J A. Epitaxial electrodeposition of Cu(111) onto an L-cysteine self-assembled monolayer on Au(111) and epitaxial lift-off of single-crystal-like Cu foils for flexible electronics[J]. J. Phys. Chem. C, 2020, 124(39): 21426-21434.

[48] Chen Q Z, Switzer J A. Electrodeposition of nanometer-thick epitaxial films of silver onto single-crystal silicon wafers[J]. J. Mater. Chem. C, 2019, 7(6): 1720-1725.

[49] Switzer J A, Liu R, Bohannan E W, Ernst F. Epitaxial electrodeposition of a crystalline metal oxide onto single-crystalline silicon[J]. J. Phys. Chem. B, 2002, 106(48): 12369-12372.

[50] Switzer J A, Kothari H M, Bohannan E W. Thermodynamic to kinetic transition in epitaxial electrodeposition [J]. J. Phys. Chem. B, 2002, 106(16): 4027-4031.

[51] Nakanishi S, Lu G T, Kothari H M, Bohannan E W, Switzer J A. Epitaxial electrodeposition of Prussian blue thin films on single-crystal Au(110)[J]. J. Am. Chem. Soc., 2003, 125(49): 14998-14999.

[52] Gudavarthy R V, Gorantla S, Mu G J, Kulp E A, Gemming T, Eckert J, Switzer J A. Epitaxial electrodeposition of Fe_3O_4 on single-crystal Ni(111)[J]. Chem. Mater., 2011, 23(8): 2017-2019.

[53] Kelso M V, Tubbesing J Z, Chen Q Z, Switzer J A. Epitaxial electrodeposition of chiral metal surfaces on silicon (643)[J]. J. Am. Chem. Soc., 2018, 140(46): 15812-15819.

[54] Vertegel A A, Bohannan E W, Shumsky M G, Switzer J A. Epitaxial electrodeposition of orthorhombic α-PbO_2 on (100)-oriented single crystal Au[J]. J. Electrochem. Soc., 2001, 148(4): C253-C256.

[55] Cheng S Y, Chen G A, Chen Y Q, Huang C C. Effect of deposition potential and bath temperature on the electrodeposition of SnS film[J]. Opt. Mater., 2006, 29(4): 439-444.

[56] Govindaraju G V, Wheeler G P, Lee D, Choi K S. Methods for electrochemical synthesis and photoelectrochemical characterization for photoelectrodes[J]. Chem. Mater., 2017, 29(1): 355-370.

[57] Leistner K, Duschek K, Zehner J, Yang M Z, Petr A, Nielsch K, Kavanagh K L. Role of hydrogen evolution during epitaxial electrodeposition of Fe on GaAs[J]. J. Electrochem. Soc., 2018, 165(4): H3076-H3079.

[58] Gusley R, Sentosun K, Ezzat S, Coffey K R, West A C, Barmak K. Electrodeposition of epitaxial Co on Ru(0001)/Al_2O_3(0001)[J]. J. Electrochem. Soc., 2019, 166(15): D875-D881.

[59] Gabe D R. The role of hydrogen in metal electrodeposition processes[J]. J. Appl. Electrochem., 1997, 27(8): 908-915.

[60] Liu R, Bohannan E W, Switzer J A, Oba F, Ernst F. Epitaxial electrodeposition of Cu_2O films onto InP(001)[J]. Appl. Phys. Lett., 2003, 83(10): 1944-1946.

[61] Liu R, Oba F, Bohannan E W, Ernst F, Switzer J A. Shape control in epitaxial electrodeposition: Cu_2O nanocubes on InP(001)[J]. Chem. Mater., 2003, 15(26): 4882-4885.

[62] Hainey M, Robin Y, Amano H, Usami N. Pole figure analysis from electron backscatter diffraction-an effective method of evaluating fiber-textured silicon thin films as seed layers for epitaxy[J]. Appl. Phys. Express, 2019, 12 (2): 025501.

[63] Wei Y M, Fu Y C, Yan J W, Sun C F, Shi Z, Xie Z X, Wu D Y, Mao B W. Growth and shape-ordering of iron nanostructures on Au single crystalline electrodes in an ionic liquid: A paradigm of magnetostatic coupling[J]. J. Am. Chem. Soc., 2010, 132(23): 8152-8157.

[64] Fu Y C, Yan J W, Wang Y, Tian J H, Zhang H M, Xie Z X, Mao B W. *In situ* STM studies on the underpotential deposition of antimony on Au(111) and Au(100) in a $BMIBF_4$ ionic liquid[J]. J. Phys. Chem. C, 2007, 111(28): 10467-10477.

[65] Lin L G, Yan J W, Wang Y, Fu Y C, Mao B W. An *in situ* STM study of cobalt electrodeposition on Au(111) in $BMIBF_4$ ionic liquid[J]. J. Exp. Nanosci., 2006, 1(3): 269-278.

[66] Deng B, Pang Z Q, Chen S L, Li X, Meng C X, Li J Y, Liu

M X, Wu J X, Qi Y, Dang W H, Yang H, Zhang Y F, Zhang J, Kang N, Xu H Q, Fu Q, Qiu X H, Gao P, Wei Y J, Liu Z F, Peng H L. Wrinkle-free single-crystal graphene wafer grown on strain-engineered substrates[J]. ACS Nano, 2017, 11(12): 12337-12345.

[67] Geiss R H, Read D T, Seiler D G, Diebold A C, McDonald R, Garner C M, Herr D, Khosla R P, Secula E M. Need for standardization of EBSD measurements for microstructural characterization of thin film structures[M]. USA: AMER INST PHYSICS, 2007.

[68] Cachet H, Cortes R, Froment M, Maurin G. Epitaxial electrodeposition of cadmium selenide thin films on indium phosphide single crystal[J]. J. Solid State Electrochem., 1997, 1(1): 100-107.

[69] Munford M L, Cortes R, Allongue P. The preparation of ideally ordered flat H-Si(111) surfaces[J]. Sens. Mater., 2001, 13(5): 259-269.

[70] Munford M L, Maroun F, Cortes R, Allongue P, Pasa A A. Electrochemical growth of gold on well-defined vicinal H-Si(111) surfaces studied by AFM and XRD[J]. Surf. Sci., 2003, 537(1-3): 95-112.

[71] Prod′homme P, Maroun F, Cortes R, Allongue P. Electrochemical growth of ultraflat Au(111) epitaxial buffer layers on H-Si(111)[J]. Appl. Phys. Lett., 2008, 93(17): 171901.

[72] Warren S, Prod′homme P, Maroun F, Allongue P, Cortes R, Ferrero C, Lee T L, Cowie B C C, Walker C J, Ferrer S, Zegenhagen J. Electrochemical Au deposition on stepped Si(111)-H surfaces: 3D versus 2D growth studied by AFM and X-ray diffraction[J]. Surf. Sci., 2009, 603(9): 1212-1220.

[73] Prodhomme P, Warren S, Cortes R, Jurca H F, Maroun F, Allongue P. Epitaxial growth of gold on H-Si(111): The determining role of hydrogen evolution[J]. Chem. Phys. Chem., 2010, 11(13): 2992-3001.

[74] Akhtari-Zavareh A, Li W J, Maroun F, Allongue P, Kavanagh K L. Improved chemical and electrical stability of gold silicon contacts via epitaxial electrodeposition[J]. J. Appl. Phys., 2013, 113(6): 063708.

[75] Zambelli T, Munford M L, Pillier F, Bernard M C, Allongue P. Cu electroplating on H-terminated n-Si(111)-properties and structure of n-Si/Cu junctions[J]. J. Electrochem. Soc., 2001, 148(9): C614-C619.

[76] Xin X, Ito K, Dutta A, Kubo Y. Dendrite-free epitaxial growth of lithium metal during charging in Li-O_2 batteries [J]. Angew. Chem. Int. Ed., 2018, 57(40): 13206-13210.

[77] Zheng J X, Zhao Q, Tang T, Yin J F, Quilty C D, Renderos G D, Liu X T, Deng Y, Wang L, Bock D C, Jaye C, Zhang D H, Takeuchi E S, Takeuchi K J, Marschilok A C, Archer L A. Reversible epitaxial electrodeposition of metals in battery anodes[J]. Science, 2019, 366(6465): 645-648.

[78] Zhang K, Yan Z H, Chen J. Electrodeposition accelerates metal-based batteries[J]. Joule, 2020, 4(1): 10-11.

[79] Chappert C, Fert A, Van Dau F N. The emergence of spin electronics in data storage[J]. Nat. Mater., 2007, 6(11): 813-823.

[80] Gundel A, Cagnon L, Gomes C, Morrone A, Schmidt J, Allongue P. In-situ magnetic measurements of electrodeposited ultrathin Co, Ni and Fe/Au(111) layers[J]. Phys. Chem. Chem. Phys., 2001, 3(16): 3330-3335.

[81] Di N, Damian A, Maroun F, Allongue P. Influence of potential on the electrodeposition of Co on Au(111) by *in situ* STM and reflectivity measurements[J]. J. Electrochem. Soc., 2016, 163(12): D3062-D3068.

[82] Cagnon L, Gundel A, Devolder T, Morrone A, Chappert C, Schmidt J E, Allongue P. Anion effect in Co/Au(111) electrodeposition: Structure and magnetic behavior[J]. Appl. Surf. Sci., 2000, 164: 22-28.

[83] Jurca H F, Damian A, Gougaud C, Thiaudiere D, Cortes R, Maroun F, Allongue P. Epitaxial electrodeposition of Fe on Au(111): Structure, nucleation, and growth mechanisms[J]. J. Phys. Chem. C, 2016, 120(29): 16080-16089.

[84] Borges J G, Prod′homme P, Maroun F, Cortes R, Geshev J, Schmidt J E, Allongue P. Perpendicular anisotropy in electrodeposited Au/Co films[J]. Phys. B: Condensed Matter, 2006, 384(1-2): 138-140.

[85] He Z, Gudavarthy R V, Koza J A, Switzer J A. Room-temperature electrochemical reduction of epitaxial magnetite films to epitaxial iron films[J]. J. Am. Chem. Soc., 2011, 133(32): 12358-12361.

[86] He Z, Koza J A, Liu Y C, Chen Q Z, Switzer J A. Room-temperature electrochemical reduction of epitaxial Bi_2O_3 films to epitaxial Bi films[J]. RSC Adv., 2016, 6(99): 96832-96836.

[87] Chen L C, Dong J W, Schultz B D, Palmstrom C J, Berezovsky J, Isakovic A, Crowell P A, Tabat N. Epitaxial ferromagnetic metal/GaAs(100) heterostructures[J]. J. Vac. Sci. Technol. B, 2000, 18(4): 2057-2062.

[88] Bao Z L, Kavanagh K L. Epitaxial Fe/GaAs via electrochemistry[J]. J. Appl. Phys., 2005, 98(6): 066103.

[89] Norton D P. Synthesis and properties of epitaxial electronic oxide thin-film materials[J]. Mater. Sci. Eng. R Rep., 2004, 43(5-6): 139-247.

[90] Pauporte T, Lincot D. Heteroepitaxial electrodeposition of zinc oxide films on gallium nitride[J]. Appl. Phys. Lett.,

1999, 75(24): 3817-3819.

[91] Pauporte T, Lincot D. Electrodeposition of semiconductors for optoelectronic devices: results on zinc oxide[J]. Electrochim. Acta, 2000, 45(20): 3345-3353.

[92] Richardson T J, Slack J L, Rubin M D. Electrochromism in copper oxide thin films[J]. Electrochim. Acta, 2001, 46 (13-14): 2281-2284.

[93] Switzer J A, Kothari H M, Poizot P, Nakanishi S, Bohannan E W. Enantiospecific electrodeposition of a chiral catalyst[J]. Nature, 2003, 425(6957): 490-493.

[94] Bohannan E W, Nicic I M, Kothari H A, Switzer J A. Enantiospecific electrodeposition of chiral CuO films on Cu(110) from aqueous Cu(II) tartrate and amino acid complexes[J]. Electrochim. Acta, 2007, 53(1): 155-160.

[95] Kothari H M, Kulp E A, Boonsalee S, Nikiforov M P, Bohannan E W, Poizot P, Nakanishi S, Switzer J A. Enantiospecific electrodeposition of chiral CuO Films from copper(II) complexes of tartaric and amino acids on single-crystal Au(001)[J]. Chem. Mater., 2004, 16(22): 4232-4244.

[96] Gudavarthy R V, Burla N, Kulp E A, Limmer S J, Sinn E, Switzer J A. Epitaxial electrodeposition of chiral CuO films from copper(II) complexes of malic acid on Cu(111) and Cu(110) single crystals[J]. J. Mater. Chem., 2011, 21 (17): 6209-6216.

[97] Brandt I S, Tumelero M A, Pelegrini S, Zangari G, Pasa A A. Electrodeposition of Cu_2O: Growth, properties, and applications[J]. J. Solid State Electrochem., 2017, 21(7): 1999-2020.

[98] Oba F, Ernst F, Yu Y S, Liu R, Kothari M, Switzer J A. Epitaxial growth of cuprous oxide electrodeposited onto semiconductor and metal substrates[J]. J. Am. Ceram. Soc., 2005, 88(2): 253-270.

[99] Wee S H, Huang P S, Lee J K, Goyal A. Heteroepitaxial Cu_2O thin film solar cell on metallic substrates[J]. Sci. Rep., 2015, 5: 16272.

[100] Switzer J A, Gudavarthy R V, Kulp E A, Mu G J, He Z, Wessel A J. Resistance switching in electrodeposited magnetite superlattices[J]. J. Am. Chem. Soc., 2010, 132 (4): 1258-1260.

[101] Grunberg P A. Nobel Lecture: From spin waves to giant magnetoresistance and beyond[J]. Rev. Mod. Phys., 2008, 80(4): 1531-1540.

[102] Switzer J A, Shane M J, Phillips R J. Electrodeposited ceramic superlattices[J]. Science, 1990, 247(4941): 444-446.

[103] Spanger B, Schiessl U, Lambrecht A, Böttner H, Tacke M. Near-room-temperature operation of $Pb_{1-x}Sr_xSe$ infrared diode lasers using molecular beam epitaxy growth techniques [J]. Appl. Phys. Lett., 1988, 53(26): 2582-2583.

[104] Johnson T H. Lead salt detectors and arrays: PbS and PbSe[J]. P. Soc. Photo-Opt. Inst., 1984(443): 60-94.

[105] Vertegel A A, Shumsky M G, Switzer J A. Epitaxial electrodeposition of lead sulfide on (100)-oriented single-crystal gold[J]. Angew. Chem. Int. Ed., 1999, 38(21): 3169-3171.

[106] Beaunier L, Cachet H, Froment M. Epitaxial electrodeposition of lead selenide films on indium phosphide single crystals[J]. Mater. Sci. Semicond. Process., 2001, 4(5): 433-436.

[107] Beaunier L, Cachet H, Cortes R, Froment M. Epitaxial electrodeposition of lead telluride films on indium phosphide single crystals[J]. J. Electroanal. Chem., 2002, 532(1-2): 215-218.

[108] Boonsalee S, Gudavarthy R V, Bohannan E W, Switzer J A. Epitaxial electrodeposition of tin(II) sulfide nanodisks on single-crystal Au(100)[J]. Chem. Mater., 2008, 20(18): 5737-5742.

[109] Brownson J R S, Georges C, Larramona G, Jacob A, Delatouche B, Lévy-Clément C. Chemistry of tin monosulfide (δ-SnS) electrodeposition: Effects of pH and temperature with tartaric acid[J]. J. Electrochem. Soc., 2008, 155(1): D40-D46.

[110] Shi D, Adinolfi V, Comin R, Yuan M J, Alarousu E, Buin A, Chen Y, Hoogland S, Rothenberger A, Katsiev K, Losovyj Y, Zhang X, Dowben P A, Mohammed O F, Sargent E H, Bakr O M. Low trap-state density and long carrier diffusion in organolead trihalide perovskite single crystals[J]. Science, 2015, 347(6221): 519-522.

[111] Dong Q F, Fang Y J, Shao Y C, Mulligan P, Qiu J, Cao L, Huang J S. Electron-hole diffusion lengths > 175 μm in solution-grown $CH_3NH_3PbI_3$ single crystals[J]. Science, 2015, 347(6225): 967-970.

[112] Banik A, Tubbesing J Z, Luo B, Zhang X T, Switzer J A. Epitaxial electrodeposition of optically transparent hole-conducting CuI on n-Si(111)[J]. Chem. Mater., 2021, 33(9): 3220-3227.

[113] Wijeyasinghe N, Eisner F, Tsetseris L, Lin Y H, Seitkhan A, Li J H, Yan F, Solomeshch O, Tessler N, Patsalas P, Anthopoulos T D. p-Doping of copper(I) thiocyanate (CuSCN) hole-transport layers for high-performance transistors and organic solar cells[J]. Adv. Funct. Mater., 2018, 28(31): 1802055.

电子功能外延薄膜的电沉积

黄 葵[1],黄容姣[1],刘素琴[1,2],何 震[1,2*]

(1. 中南大学化学化工学院,湖南 长沙 410083; 2. 化学电源湖南省重点实验室,湖南 长沙 410083)

摘要: 电沉积作为一种在温和条件下从溶液中合成材料的技术已被广泛应用于在导体和半导体基底表面合成各种功能材料。电沉积一般由人为施加于基底的电刺激(如:施加电位/电流)来触发。这种电刺激通过氧化或还原靠近基底表面的溶液层内部的离子、分子或配合物从而使该溶液层偏离其热力学平衡状态, 随后引起目标产物在基底表面的沉积。在电沉积过程中, 许多实验参数都可能从不同的方面对沉积物的物化性质造成影响。迄今为止,已通过电沉积制备出多种单质(包括金属和非金属单质)、化合物(例如:金属氧化物、金属氢氧化物、金属硫化物等)以及复合材料。电沉积制备的这些材料大多为多晶、织构或外延薄膜的形式。其中, 外延薄膜是一种具有特定的面外和面内晶体生长取向且其晶体取向受基底控制的类单晶薄膜。由于外延薄膜中高度有序的原子排列,它们常呈现出独特的电磁性质。本文总结了常见的电沉积合成路线及影响沉积物外延生长的关键实验因素。此外, 本文简要介绍了用于表征外延薄膜的技术。最后, 本文还讨论了一些采用电沉积制备的具有特殊电子、电磁及光电特性的功能外延薄膜。

关键词: 电沉积;电镀;薄膜;高度定向